UNIVERSIDADE FEDERAL DA INTEGRAÇÃO LATINO-AMERICANA

PROGRAMA DE PÓS GRADUAÇÃO EM FÍSICA APLICADA

Raul Vinícius Basso Morás

Analysis of the Fluctuation-Dissipation Theorem and Memory Effects in Thermodynamic Systems under the Influence of External Forces

Foz do Iguaçu

2025

Raul Vinícius Basso Morás

Analysis of the Fluctuation-Dissipation Theorem and Memory Effects in Thermodynamic Systems under the Influence of External Forces

Master's Dissertation presented to the *Programa de Pós-Graduação em Física Aplicada* at the *Universidade Federal da Integração Latino-Americana* as a partial requirement for obtaining the title of Master in Physics.

Universidade Federal da Integração Latino-Americana

Supervisor: Luciano Calheiros Lapas

Foz do Iguaçu

2025

Raul Vinícius Basso Morás

Analysis of the Fluctuation-Dissipation Theorem and Memory Effects in Thermodynamic Systems under the Influence of External Forces

Master's Dissertation presented to the *Programa de Pós-Graduação em Física Aplicada* at the *Universidade Federal da Integração Latino-Americana* as a partial requirement for obtaining the title of Master in Physics.

Grade: _____

Foz do Iguaçu, January 14, 2025.

EXAMINING BOARD

Luciano Calheiros Lapas - Supervisor
UNILA

Maria Florencia Carusela
UNGS

Rafael Morgado Silva
UnB

Catalogação elaborada pelo Setor de Tratamento da Informação
Catalogação de Publicação na Fonte. UNILA - BIBLIOTECA LATINO-AMERICANA - CENTRAL

B322a
Basso Morás, Raul Vinícius.
Analysis of the fluctuation-dissipation theorem and memory effects in thermodynamic systems under the Influence of external forces / Raul Vinícius Basso Morás. - Foz do Iguaçu, 2025.
87 fls.: il.

Universidade Federal da Integração Latino-Americana, Centro interdisciplinar de Ciências da Natureza, Programa de pós-graduação em física aplicada.
Orientador: Luciano Calheiros Lapas.

1. Brownian motion processes. 2. Langevin equations. 3. Fluctuations (Physics). I. Lapas, Luciano Calheiros. II. Título.

CDU 536

Acknowledgements

I would like to thank, first and foremost, my parents, Nadjanara and Janderson, for their unconditional support throughout my journey. Thank you for encouraging me to pursue Physics, supporting me in moving to a new city, starting my master's program, and for always being by my side, day after day. Without you, none of this would have been possible.

To my family, especially my grandparents, I extend my heartfelt gratitude. Grandma Mari and Grandpa Edemar, from you I learned that love and support from those close to us are the foundation of true happiness. Grandma Nina and Grandpa José, from you I learned that hard work always brings results.

I am deeply grateful to Professor Florencia Carusela for everything I learned under her guidance. In addition to being an excellent professional, she conducted my work with care and dedication, and the good results are a reflection of her commitment.

To my close friends, Camila, Lucas, and Miguel, my gratitude for making life lighter and happier. With you, I feel comfortable being who I truly am.

I also want to thank my brother Totty, the brother life gave me. You have always been, always are, and always will be by my side, and I am immensely grateful for that.

This work was made possible thanks to the computational support provided by UNGS and LCAD-UNILA, as well as financial support from CAPES and CNPq.

Finally, to my advisor, thank you for your guidance not only in my master's project but also in life. Thank you for all your patience and dedication. Your mentorship is an inspiration that I will carry with me throughout my life.

"When we are in love, we always want to tell the world. That passion is the essence of science: we want to share what we have discovered."

(Carl Sagan)

"If I could wish for anything, I would not wish for wealth or power, but the passion for possibility; I would wish only for an eye that, eternally young, burns with the desire to see possibility."

(Soren Kierkegaard)

Abstract

Every body with a finite temperature emits electromagnetic radiation in the form of photons. Heat transfer by radiation is, therefore, a fundamental property widely studied in thermodynamics and statistical physics [1, 2, 3]. In the near-field regime, where distances are on the order of or smaller than the characteristic thermal wavelength (λ_T), additional significant effects emerge, such as the contribution of evanescent waves and short-range field fluctuations [4, 5]. Under these conditions, radiative heat transfer can considerably exceed the limits predicted by the Stefan-Boltzmann Law, requiring an approach grounded in non-equilibrium thermodynamics and quantum electrodynamics. To adequately describe such phenomena, the formalism of the generalized Langevin equation [6, 7, 8, 9] emerges as a powerful tool, as it allows modeling the dynamics of systems with memory and temporal correlations, enabling the analysis of transport processes out of thermal equilibrium. The present work aims to investigate phenomena associated with the anomalous diffusion regime and its possible connections with anomalous heat transfer in out-of-equilibrium systems.

The results obtained encompass both theoretical and computational approaches. The transient and asymptotic behaviors of the Fluctuation-Dissipation Theorem, in its normal and generalized forms, were analyzed in detail under the influence of an external force. In this context, the properties of the external force and the relaxation function were investigated, demonstrating for which systems the theorem remains valid and for which an asymptotic correction is required, with the nature of this correction explicitly detailed. Additionally, the effective temperature was determined from the density of states, with results ranging between the thermal bath temperature and the system's initial temperature, depending on the diffusion regime (normal or ballistic). Computational simulations corroborated these predictions, demonstrating the model's applicability to a wide range of dynamic scenarios. In the context of Brownian motion simulations, the generalized Langevin equation was solved numerically, with validation of the model in normal and ballistic diffusion regimes. Furthermore, a linear relationship was identified between the kinetic and effective temperatures. The introduction of confinement in nanometric boxes revealed that reduced volumes favor the preservation of the system's initial memory. Finally, in simulations involving evanescent waves, a stabilization of temperature at values higher than those of the thermal bath was observed, attributed to the presence of an external electric field. This behavior was associated with long-term memory preservation and continuous energy dissipation, suggesting new perspectives for the study of out-of-equilibrium systems.

Keywords: Brownian motion, near-field regime, generalized Langevin equation, fluctuation-dissipation theorem

Resumo

Todo corpo com temperatura finita emite radiação eletromagnética na forma de fótons. A transferência de calor por irradiação é, portanto, uma propriedade fundamental amplamente estudada em termodinâmica e física estatística [1, 2, 3]. No regime de campo próximo, em que as distâncias são da ordem ou menores que o comprimento de onda térmico característico (λ_T), emergem efeitos adicionais significativos, como a contribuição de ondas evanescentes e as flutuações de campos de curto alcance [4, 5]. Nestas condições, a transferência radiativa de calor pode exceder consideravelmente os limites previstos pela Lei de Stefan-Boltzmann, demandando uma abordagem fundamentada na termodinâmica de não equilíbrio e na eletrodinâmica quântica. Para descrever adequadamente tais fenômenos, o formalismo da equação de Langevin generalizada [6, 7, 8, 9] apresenta-se como uma ferramenta poderosa, pois permite modelar a dinâmica de sistemas com memória e correlações temporais, viabilizando a análise de processos de transporte fora do equilíbrio térmico. O presente trabalho tem como objetivo investigar fenômenos associados ao regime de difusão anômala e suas possíveis conexões com a transferência anômala de calor em sistemas fora do equilíbrio.

Os resultados obtidos abrangem tanto abordagens teóricas quanto computacionais. Foram analisados, em detalhe, os comportamentos transientes e assintóticos do Teorema de Flutuação-Dissipação, em suas formas normal e generalizada, sob a influência de uma força externa. Neste contexto, investigaram-se as propriedades da força externa e da função de relaxação, demonstrando-se para quais sistemas o teorema permanece válido e para quais é necessária uma correção assintótica, explicitando-se a natureza dessa correção. Adicionalmente, determinou-se a temperatura efetiva a partir da densidade de estados, com resultados que variam entre a temperatura do banho térmico e a temperatura inicial do sistema, a depender do regime de difusão (normal ou balístico). Simulações computacionais corroboraram estas previsões, evidenciando a aplicabilidade do modelo em uma ampla gama de cenários dinâmicos. No contexto das simulações do movimento browniano, a equação de Langevin generalizada foi resolvida numericamente, com validação do modelo nos regimes de difusão normal e balística. Identificou-se, ainda, uma relação linear entre as temperaturas cinética e efetiva. A introdução de confinamento em caixas nanométricas revelou que volumes reduzidos favorecem a preservação da memória inicial do sistema. Por fim, nas simulações envolvendo ondas evanescentes, observou-se uma estabilização da temperatura em valores superiores aos do banho térmico, atribuída à presença de um campo elétrico externo. Esse comportamento foi associado à preservação de memória de longo prazo e à dissipação energética contínua, sugerindo novas perspectivas para o estudo de sistemas fora do equilíbrio.

Palavras-chave: Movimento browniano, regime de campo próximo, equação de Langevin generalizada, teorema de flutuação dissipação.

Resumen

Todo cuerpo con temperatura finita emite radiación electromagnética en forma de fotones. La transferencia de calor por radiación es, por lo tanto, una propiedad fundamental ampliamente estudiada en termodinámica y física estadística [1, 2, 3]. En el régimen de campo cercano, donde las distancias son del orden o menores que la longitud de onda térmica característica (λ_T), surgen efectos adicionales significativos, como la contribución de ondas evanescentes y las fluctuaciones de campos de corto alcance [4, 5]. En estas condiciones, la transferencia radiativa de calor puede exceder considerablemente los límites previstos por la Ley de Stefan-Boltzmann, lo que requiere un enfoque basado en la termodinámica de no equilibrio y la electrodinámica cuántica. Para describir adecuadamente dichos fenómenos, el formalismo de la ecuación de Langevin generalizada [6, 7, 8, 9] se presenta como una herramienta poderosa, ya que permite modelar la dinámica de sistemas con memoria y correlaciones temporales, facilitando el análisis de procesos de transporte fuera del equilibrio térmico. El presente trabajo tiene como objetivo investigar fenómenos asociados al régimen de difusión anómala y sus posibles conexiones con la transferencia anómala de calor en sistemas fuera del equilibrio.

Los resultados obtenidos abarcan tanto enfoques teóricos como computacionales. Se analizaron en detalle los comportamientos transitorios y asintóticos del Teorema de Fluctuación-Disipación, en sus formas normal y generalizada, bajo la influencia de una fuerza externa. En este contexto, se investigaron las propiedades de la fuerza externa y de la función de relajación, demostrando para qué sistemas el teorema permanece válido y para cuáles es necesaria una corrección asintótica, explicitándose la naturaleza de dicha corrección. Además, se determinó la temperatura efectiva a partir de la densidad de estados, con resultados que varían entre la temperatura del baño térmico y la temperatura inicial del sistema, dependiendo del régimen de difusión (normal o balístico). Las simulaciones computacionales corroboraron estas predicciones, evidenciando la aplicabilidad del modelo en una amplia gama de escenarios dinámicos. En el contexto de las simulaciones del movimiento browniano, la ecuación de Langevin generalizada se resolvió numéricamente, con validación del modelo en los regímenes de difusión normal y balística. Asimismo, se identificó una relación lineal entre las temperaturas cinética y efectiva. La introducción de confinamiento en cajas nanométricas reveló que volúmenes reducidos favorecen la preservación de la memoria inicial del sistema. Finalmente, en las simulaciones que involucran ondas evanescentes, se observó una estabilización de la temperatura en valores superiores a los del baño térmico, atribuida a la presencia de un campo eléctrico externo. Este comportamiento se asoció con la preservación de la memoria a largo plazo y la disipación energética continua, sugiriendo nuevas perspectivas para el estudio de sistemas fuera del equilibrio.

Palabras clave: Movimiento browniano, régimen de campo cercano, ecuación de Langevin generalizada, teorema de fluctuación-disipación.

List of Figures

List of Tables

List of abbreviations and acronyms

GLE	Generalized Langevin Equation
FDT	Fluctuation-Dissipation Theorem
FPE	Fokker-Planck Equation
OLR	Onsager's Linear Relation
MEMS	Microelectromechanical Systems
NEMS	Nanoelectromechanical Systems
EH	Ergodic Hypothesis
NLE	Normal Langevin Equation
OU	Ornstein-Uhlenbeck process
W	Wiener process

List of symbols

e_b	Power radiated per unit of area by a black body
σ	Stefan-Boltzmann constant
T	Temperature
λ_T	Characteristic thermal wavelength
$\hbar$	Reduced Planck constant
c	Speed of light
k_B	Boltzmann constant
x	Position
t	Time
D	Diffusion coefficient
m	Mass
v	Particle's velocity
γ	Friction coefficient
$\xi(t)$	Random force
$\delta(t)$	Dirac delta function
α	Diffsion expoent
$R(t)$	Response function
N	Number of interacting particles
V	System's volume
E_j	Energy microstate
E_0	System's total energy
A_N	Normalization factor
Ω	Number of microstates

P_j	Probability of a given microstate
β	Inverse temperature
q	Generalized position
p	Generalized momentum
$\mathcal{H}$	System's Hamiltonian
$V(q)$	Potential energy function
$\rho(q,p)$	Phase space distribution function
$\hat{X}$	Pertubative term
$Y(q,p)$	Conjugate moment
$\Lambda_{A,\hat{X}}$	Generalized susceptibility
$\mathscr{L}$	Liouville operator
$f(q,p,t)$	Boltzmann's distribution function
$H(t)$	Boltzmann's H function
S	Entropy
F_{ext}	External force
A	Canonical momentum
D_T	Noise intensity
$\mathcal{L}$	Laplace transform
$C_A(t)$	Autocorrelation of the Canonical momentum
Cov	Covariance
σ_A	Variance of the Canonical momentum
Λ_T	Correction Term of the Fluctuation-Dissipation Theorem
β_F	Exponential Coefficient of the External Force
ω	Angular frequency
$\Gamma(t-t')$	Memory function
$\tilde{R}(z)$	Relaxation function

$C_\xi(t)$	Autocorrelation of the stochastic noise
$A^\dagger(t)$	Renormalization of the Canonical momentum
$R_0(t)$	Response function in the presence of an external force
c_T	Positive constante
$T_{ef.}$	Effective Temperature
T_0	Initial temperature
T_R	Reservoir Temperature
$E(x,z)$	Electric field
k_i	Wave vector
$S(\omega)$	Power spectrum
M_ω	Integral that Determines the Behavior of $R(t)$
q_e	Electric Charge
$A^{(R)}$	Coulomb constant
$B^{(A)}$	Elastic constant

Contents

1 Introduction

Every body with finite temperature emits electromagnetic radiation in the form of photons, and heat transfer by radiation is a fundamental property studied in thermodynamics and statistical physics. Understanding this process was a significant challenge in the 19th and 20th centuries, culminating in the development of quantum theory. In 1879, Josef Stefan [1], based on experimental results, and, in 1884, Ludwig Boltzmann [2], through theoretical derivation, established that the power radiated per unit area, e_b, of a black body is proportional to the fourth power of its absolute temperature, T. This relationship, known as the *Stefan-Boltzmann Law*, is expressed by:

$$e_b = \sigma T^4, \tag{1.1}$$

where σ is the Stefan-Boltzmann constant. Later, in 1900, Max Planck [3] proposed a formula for the spectral density of black-body radiation, introducing the concept of energy quantization and resolving the "ultraviolet catastrophe" problem. Planck's formulation not only corroborated the Stefan-Boltzmann Law but also laid the foundation for the emergence of quantum mechanics.

However, the validity of the Stefan-Boltzmann Law is limited to the far-field regime, where the distances between the emitting and receiving surfaces are much larger than the characteristic thermal wavelength, $\lambda_T = \hbar c/k_B T$, where $\hbar$ is the reduced Planck constant, c is the speed of light, k_B is the Boltzmann constant, and T is the temperature. Exploring the near-field regime, where distances are on the order of or smaller than λ_T, reveals additional effects such as the contribution of evanescent waves and short-range field fluctuations [4, 5]. In these cases, radiative heat transfer can significantly exceed the limits predicted by the Stefan-Boltzmann Law, requiring a description based on non-equilibrium thermodynamics and quantum electrodynamics.

The formalism of the generalized Langevin equation [6, 7, 8, 9] provides a powerful tool for describing the dynamics of systems with memory and temporal correlations, enabling the analysis of transport processes in systems out of thermal equilibrium. In this context, memory effects and correlations between system and reservoir fluctuations can lead to anomalous diffusion behaviors and unconventional energy transfer. Diffusive systems described by this formalism depend on the density of states of the thermal reservoirs, and in cases of strong correlation, the resulting dynamics can exhibit significant deviations from classical diffusion laws [10, 11].

In this work, we will investigate phenomena associated with the anomalous diffusion regime, exploring possible connections with anomalous heat transfer in non-equilibrium systems. Specifically, we aim to understand how temporal correlations influence energy

transport processes and how these can be described within the generalized Langevin formalism. We expect that this approach will contribute to a deeper understanding of the underlying mechanisms of heat transfer at the nanoscale and in materials with unconventional properties.

1.1 Brownian Motion

Brownian motion is characterized as the random and continuous motion of microscopic particles suspended in a fluid, whether liquid or gas. This phenomenon was first described by the Scottish botanist Robert Brown in 1827 [12], who observed under a microscope the irregular behavior of pollen grains in aqueous suspension. Brown noted that the particles appeared to move erratically, without any discernible direction or pattern.

Before the development of modern theory, other scientists also investigated the phenomenon. In 1863, Christian Wiener [13] made an important contribution by concluding that the origin of the motion was not associated with interparticle forces, temperature variations in the fluid, or the evaporation process. Two years later, in 1865, Cantoni and Oehl conducted a year-long observational study, confirming that the motion of particles in a fluid sealed between glass plates did not depend on external conditions, suggesting an intrinsic origin to the system.

The detailed and quantitative theoretical understanding of Brownian motion was developed by Albert Einstein in 1905 [14]. In this seminal work, Einstein established the relationship between Brownian motion and the kinetic theory of gases, providing an explanation based on the microscopic behavior of the fluid's constituent molecules. He demonstrated that the motion of suspended particles results from incessant collisions with the medium's molecules, culminating in the formulation of a mathematical relationship that describes the mean squared displacement of these particles over time,

$$\langle x^2(t)\rangle = 2Dt,$$

where $\langle x^2(t)\rangle$ is the mean squared displacement[1], D is the diffusion coefficient, and t is time. Einstein's analysis was crucial for corroborating the existence of atoms and molecules, establishing itself as a milestone in statistical physics and providing the foundation for studying diffusive processes in microscopic systems.

Simultaneously, Marian Smoluchowski [15] independently developed a similar theory, reinforcing Einstein's results. Subsequently, in 1908, Paul Langevin [16] presented a different approach by introducing a stochastic differential equation that describes the dynamics of Brownian motion, known as the Langevin equation. This equation explicitly considers the

[1] The symbol $\langle\cdots\rangle$ represents an ensemble average.

random forces and drag force acting on the particle,

$$m\frac{dv}{dt} = -\gamma v + \sqrt{2\gamma k_B T}\,\xi(t),$$

where m is the particle mass, v is its velocity, γ is the friction coefficient, and $\xi(t)$ is a random force with zero mean and a correlation expressed as a Dirac delta function, $\delta(t)$. Here T is the absolute temperature of the thermal bath in equilibrium.

The rigorous mathematical formalism of Brownian motion was developed by Norbert Wiener [17], leading to the concept of the *Wiener process*, fundamental in probability theory and stochastic processes. Brownian motion thus became an essential tool in various fields such as physics, chemistry, biology, and finance, being used to model a wide range of phenomena.

Moreover, the study of Brownian motion and diffusive processes led to the development of theories of anomalous diffusion, where the mean squared displacement is not linear in time but follows a law of the form $\langle x^2(t)\rangle \propto t^\alpha$, with the diffusion exponent $\alpha \neq 1$. These phenomena are relevant in complex systems, disordered media, and at nanoscopic scales, where interactions and spatial constraints significantly influence particle dynamics [10, 11].

In this context, Brownian motion is not only fundamental to understanding typified diffusive processes, such as Einstein diffusion, but also serves as a starting point for studying more complex dynamics, such as subdiffusive ($0 < \alpha < 1$) and superdiffusive ($1 < \alpha \leq 2$) diffusion, where $\alpha = 2$ represents ballistic diffusion. Exploring these anomalous regimes has significant implications for understanding phenomena such as transport in biological materials, polymer dynamics, and nanoscale heat transfer [18].

From the stochastic description of microscopic particle motion, it is understood that the dynamics of these particles contain fundamental information about thermodynamics. In equilibrium systems, a well-defined thermodynamics can be developed based on these principles, assuming certain conditions, such as infinitesimal variations in system variables and the non-negativity of entropy production [19]. Under these premises, processes such as heat exchange and thermodynamic quantities, like temperature, can be rigorously defined through the fluctuation-dissipation theorem [20, 21]. In this context, heat is lost through fluctuations and gained through dissipation, allowing the rigorous formulation of system temperature.

However, for systems out of equilibrium, where variables exhibit widely differing time scales, the fluctuation-dissipation theorem in its classical form, without considering memory effects, becomes inadequate, making it impossible to precisely define temperature [22]. To describe such systems, the use of non-equilibrium thermodynamics [23, 24] becomes necessary. Approaches to this include generalizing the fluctuation-dissipation theorem itself, utilizing, for instance, equations such as the Fokker-Planck equation or Onsager's

linear relations, which aim to describe the thermodynamic behavior of non-equilibrium systems [25, 26].

1.2 Near-Field Regime

In the late 1960s and early 1970s, pioneering experiments conducted by Hargreaves [27], Domoto, Boehm, and Tien [28, 29] began to reveal the phenomenon of enhanced radiative heat transfer in the near-field regime. They observed that when two surfaces were brought closer to distances smaller than λ_T, there was a significant increase in thermal conductance.

In 1971, Polder and van Hove [4], building on Rytov's fluctuational electrodynamics theory [30, 31], developed a theoretical approach to calculate radiative heat transfer by distinguishing the radiation contributions described by the Stefan-Boltzmann Law from the unique characteristics of the near-field regime. Their methodology was based on the fluctuation-dissipation theorem, focusing on the interaction between two bodies via dipole interactions. As the random motion of these particles (fluctuations) occurs, variations in the electromagnetic field are generated, resulting in energy transfer to the second body, leading to dissipation and an exacerbated heat flux.

The discovery of radiative heat transfer at nanometric distances revolutionized the understanding of the limits established by the Stefan-Boltzmann Law, inaugurating a new research area in thermal science and nanotechnology. Since then, numerous theoretical [32, 33, 34, 35, 36, 37, 38] and experimental [39, 40, 41, 42, 43, 44] studies have confirmed and expanded these findings. They demonstrated that when near-field effects (i.e., the collective influence of diffraction, interference, and wave tunneling) become relevant, radiative heat transfer can exceed the predictions of the Stefan-Boltzmann Law by several orders of magnitude.

Understanding anomalous heat transfer in the near-field regime is fundamental for developing a solid scientific foundation, broadening knowledge about these phenomena, and enabling the development of new technological applications [45]. Moreover, devices leveraging these characteristics are already a reality in various contexts. Near-field thermophotovoltaic systems [46, 47] exploit intensified radiative transfer to convert heat into electricity with higher efficiency. Thermal rectifiers [48, 49] and thermal transistors [50, 38] enable directional control of heat flux, paving the way for thermal information processing. Energy harvesters [51] capitalize on thermal fluctuations to generate energy at the nanoscale. Pyroelectric systems that convert near-field thermal energy provide an alternative for recovering dissipated thermal energy in industrial processes. The transmission efficiency of these systems depends on the surface separation distance, as demonstrated by Fang et al. [52], who recorded an efficiency of $6.5\,\mathrm{mW/cm^2}$ at a distance of $100\,\mathrm{nm}$.

Subsequently, Latella and Ben-Abdallah [53] achieved values of up to $130\,\mathrm{mW/cm^2}$ in graphene-based systems.

Advances in nanofabrication and metrology techniques have enabled increasingly precise control and direct observation of heat transfer at nanometer-scale distances. These advances revealed that the radiative heat flux is amplified due to the contribution of surface electromagnetic waves [54, 5]. Analogous to the control of electron flow in electrical circuits that drove modern electronics, progress in thermal systems has been made to achieve precise manipulation of heat flows. In 2002, Terraneo et al. [55] proposed a thermal rectifier model in a one-dimensional nonlinear system, followed by the proposal of a thermal diode model [56] based on the coupling of two nonlinear systems. Subsequently, the concept of a thermal transistor [57] was introduced, employing three nonlinear systems and allowing additional control over heat transfer.

Furthermore, the influence of the near-field regime extends to the study of the Casimir-Lifshitz force [58, 59], paving the way for the design of micro- and nanoelectromechanical systems (MEMS and NEMS) [60]. Exploring Casimir-Lifshitz forces, originating from vacuum quantum fluctuations in the presence of nearby surfaces, has been crucial for understanding nanoscale interactions. These forces not only affect heat transfer but also have significant implications for the mechanical behavior and stability of nanometric-scale devices [61].

Additionally, devices tailored for specific applications, such as nanodevice cooling [62] and magnetic recording devices [63, 64], have emerged. The theoretical development underlying such devices is essential, with Brownian motion dynamics offering an alternative and relevant approach for understanding these mechanisms.

This work aims to contribute to this growing research area by investigating how fluctuations and interactions of Brownian particles under the influence of evanescent waves impact the mechanisms of power transfer to the thermal reservoir. In particular, we will explore the connections between anomalous diffusion and the ballistic regime.

1.3 Presentation of the Dissertation

This work aims to contribute to the deepening of discussions on the Langevin equation, examining its theoretical evolution and practical applications in the context of Brownian motion and complex interactions. The goal is to bridge the classical description of Brownian motion with broader contemporary approaches, thereby providing a solid foundation for understanding phenomena involving fluctuations and dissipation in dynamic systems.

In **Chapter 2**, a literature review is presented, addressing the concepts of linear

response. Building on Zwanzig's theory [65], we analyze how linear response influences different thermodynamic quantities under the application of external forces. This analysis serves as a foundation for subsequent chapters, where we develop a computational model capable of simulating the behavior of a particle subjected to external electromagnetic forces — in particular, a time-oscillating evanescent wave — and interaction with a second particle via Coulomb and elastic forces.

In **Chapter 3**, we conduct an in-depth review of Langevin's approach and that of other scientists regarding the Brownian motion problem. In this context, we introduce the Langevin equation in its normal and generalized forms, discussing the associated fluctuation-dissipation theorems. Subsequently, we analyze the asymptotic behavior of both formulations under the influence of an arbitrary external force. Finally, we propose the use of the response function $R(t)$ to describe the temporal evolution of the effective temperature, extending this perspective to provide a more general understanding of the fluctuation-dissipation theorem.

In **Chapter 4**, we detail the methodological aspects of the developed model, including the resolution of the generalized Langevin integro-differential equation and the generation of an external random force. We also explore the implementation of external forces and confinement in a box, simulating the particle's position within a material lattice.

Finally, in **Chapter 5**, we present the obtained results. We begin with an analysis of well-established situations, such as normal and ballistic diffusion, and proceed to discuss the effects of confinement, interaction with the evanescent wave, and interaction with a second particle.

2 Langevin Equation

Understanding thermodynamic phenomena in many-body systems is one of the central tasks of theoretical physics. In systems composed of a large number of particles, the complexity of interactions and the variety of possible states require an approach that connects the microscopic properties of individual particles with the macroscopic behavior observed.

The development of understanding many-body systems and their connection with thermodynamics began in the late 19th and early 20th centuries, when scientists started exploring the relationships between microscopic and macroscopic properties. One of the pioneers in this field was Ludwig Boltzmann, who introduced the idea that the thermodynamic behavior of a system could be understood in terms of the statistics of its constituent particles.

The H-Theorem, derived from the Boltzmann equation, describes the temporal evolution of the particle distribution function in a dilute gas. The distribution function $f(q, p, t)$ represents the particle density in phase space, where q and p are, respectively, the position and linear momentum of the particles at a given time t. Boltzmann defined a quantity H, given by:

$$H(t) = \int dq \int dp f(q, p, t) \ln f(q, p, t).$$

According to the H-Theorem, the function $H(t)$ decreases monotonically over time, i.e., $\frac{dH(t)}{dt} \leq 0$. This decrease is associated with the increase in entropy in the system, as $H(t)$ is inversely related to entropy: the lower the value of $H(t)$, the higher the entropy S, according to the relation $S \propto -H$.

The Langevin Equation captures the essential features of Brownian motion by considering the energy dissipation due to viscous friction and thermal fluctuations represented by the random force, enabling the modeling of particle motion in complex media. This approach provides a mesoscopic description that bridges microscopic dynamics with macroscopic observables. In this sense, both formalisms (H-Theorem and Langevin) aim to describe the emergent irreversibility in physical systems based on their microscopic dynamics. While the H-Theorem uses the Boltzmann equation to address the temporal evolution of the distribution function in a dilute gas, demonstrating that the system tends to evolve toward a Maxwell-Boltzmann equilibrium distribution, the Langevin Equation provides a stochastic description of the individual motion of a particle subjected to interactions with the medium.

This methodology, which explores the dynamic behavior of particles under the influence of random forces, will be explored in detail in this chapter, highlighting how it

complements and expands the understanding provided by traditional methods of statistical physics.

2.1 Normal Langevin Equation

In its initial formulation [16], Langevin proposed that particles undergoing Brownian motion behave as classical particles subjected to two distinct types of forces. He considered that a particle of mass m and velocity $v(t)$ in a viscous fluid would be subjected to forces responsible for the motion attributed to Robert Brown [12], known as Brownian motion. The first of these forces is a viscosity force, dependent on the particle's velocity, expressed as $-m\gamma v(t)$. This term varies over a long timescale, making it a slow variable. The second force is stochastic in nature, associated with noise $\xi(t)$, characterized by short timescales and thus being a fast variable. Additionally, an external force $F_{ext}(t)$ may be included, which can act as a slow or fast variable depending on its origin and representation in the system. Thus, the conventional Langevin equation is expressed as:

$$\frac{dA}{dt} = -\gamma A + \xi(t) + F_{ext}(t), \tag{2.1}$$

where the canonical momentum is denoted by $A = mv(t)$. It is worth noting that for more complex systems, the exclusive use of canonical momentum in the equation may not suffice to fully describe the dynamics. In such cases, other dynamic quantities can be introduced into the formulation to adequately capture the phenomena involved [66]. This generalization will be explored in greater depth in the following sections, addressing situations where variables other than canonical momentum become relevant for a more comprehensive description of the systems under analysis.

In this approach, the stochastic force is considered Markovian, characterized by the absence of temporal correlation [67]. This implies that the temporal evolution of the system is *local in time*; that is, the future state depends solely on the present state, without influence from past states, so that noise fluctuations have no memory of past values. Specifically, a Markovian noise is often modeled as "white noise," where its variations are statistically independent at different time instants [68].

From a mathematical perspective, using ensemble theory and representing the statistical mean by the symbol $\langle\cdot\rangle$, the white noise $\xi(t)$ has zero mean[1],

$$\langle\xi(t)\rangle = 0, \tag{2.2}$$

and its correlation function, as established by the Fluctuation-Dissipation Theorem, is given by

$$\langle\xi(t)\xi(t')\rangle = D_T\delta(t-t'), \tag{2.3}$$

[1] Note that having a zero mean is not an exclusive characteristic of white noise. This property of noise stationarity can also be present in correlated noise.

where D_T is a constant quantifying the noise intensity, and $\delta(t-t')$ is the Dirac delta function. This form of the correlation function indicates that noise fluctuations at different times, t and t', are uncorrelated when $t \neq t'$, reinforcing the memoryless nature of the process.

Additionally, since the particle's motion is driven by fluctuations of the thermal bath in which it is immersed, and due to causality, there is no correlation between the initial configuration of the Brownian particle, $A(0)$, and the stochastic force $\xi(t)$. This lack of correlation can be expressed mathematically as

$$\langle A(0)\xi(t)\rangle = 0. \tag{2.4}$$

These properties make noise particularly useful for simplifying the dynamics of systems subject to rapid fluctuations, enabling a straightforward approach to studying stochastic phenomena.

2.2 Normal Fluctuation-Dissipation Theorem

The behavior of the momentum over time can be obtained from the solution of the Langevin Equation, which is derived using the Laplace transform of Eq. (2.1) and its inverse [69, 70],

$$A(t) = A(0)e^{-\gamma t} + \int_0^t e^{-\gamma(t-t')}\xi(t')dt' + \int_0^t e^{-\gamma(t-t')}F_{\text{ext}}(t')dt'. \tag{2.5}$$

For the terms involving $\tilde{\xi}(z)$ and $\tilde{F}_{\text{ext}}(z)$ in the Laplace domain z, we use the Laplace transform property of a derivative in the t domain [69, 70],

$$\mathcal{L}\left\{\frac{df(t)}{dt}\right\} = z\tilde{f}(z) - f(0), \tag{2.6}$$

as well as the convolution property of the Laplace transform and its inverse,

$$\mathcal{L}\left\{\int_0^t f(t-t')g(t')dt'\right\} = \tilde{f}(z)\tilde{g}(z) \quad \text{and} \quad \mathcal{L}^{-1}\left\{\tilde{f}(z)\tilde{g}(z)\right\} = \int_0^t f(t-t')g(t')\,d\tau, \tag{2.7}$$

for two arbitrary functions $f(t)$ and $g(t)$, where $\tilde{f}(z) = \mathcal{L}\{f(t)\}$ represents the Laplace transform of a function $f(t)$.

Multiplying Eq. (2.5) by $A(0)$, taking the ensemble average, and considering condition (2.4), we obtain the autocorrelation of A

$$C_A(t) = \langle A(t)A(0)\rangle = \langle A^2(0)\rangle e^{-\gamma t} + \langle A(0)\rangle \int_0^t e^{-\gamma(t-t')}F_{\text{ext}}(t')dt'. \tag{2.8}$$

The second term on the right-hand side of this equation represents the drift effect in the autocorrelation function $C_A(t)$, explicitly showing the cumulative influence of the external

force $F_{\text{ext}}(t)$ on the correlation between the initial state $A(0)$ and the state at a later time $A(t)$, weighted by the initial mean $\langle A(0)\rangle$. When the initial mean $\langle A(0)\rangle$ is nonzero, there is a direct correlation between the initial value of the variable A and its temporal evolution influenced by the external force. This means the particle exhibits a systematic drift induced by the applied external force. This drift is in addition to the system's random fluctuations and can guide the particle along a preferential trajectory.

On the other hand, in the absence of an external force or when we assume $\langle A(0)\rangle = 0$, the drift effect vanishes. In this case, the second term in Eq. (2.8) is eliminated, and the autocorrelation function simplifies to

$$C_A(t) = \langle A^2(0)\rangle e^{-\gamma t}, \tag{2.9}$$

indicating that the temporal evolution of the correlation is governed solely by random fluctuations and the exponential decay due to the dissipative term $-\gamma A$ in the Langevin equation. Thus, there is no systematic trend in the particle's motion, and the behavior is purely diffusive[2]

An alternative approach to eliminating drift effects involves computing the covariance between $A(t)$ and $A(0)$:

$$\text{Cov}[A(t), A(0)] = \langle A(t)A(0)\rangle - \langle A(t)\rangle\langle A(0)\rangle. \tag{2.10}$$

Given that the mean of $A(0)$ is simply $\langle A(0)\rangle$, and the mean of $A(t)$ is obtained from Eq. (2.5) and condition (2.2),

$$\langle A(t)\rangle = \langle A(0)\rangle e^{-\gamma t} + \int_0^t e^{-\gamma(t-t')} F_{\text{ext}}(t')dt', \tag{2.11}$$

assuming that $F_{\text{ext}}(t')$ is deterministic, substituting these results into Eq. (2.10), we have

$$\text{Cov}[A(t), A(0)] = \sigma_A^2(0)e^{-\gamma t}, \tag{2.12}$$

where $\sigma_A^2(0)$ is the variance of $A(t)$ at $t = 0$, defined as

$$\sigma_A^2 = \langle A^2(t)\rangle - \langle A(t)\rangle^2. \tag{2.13}$$

This result shows that the covariance of $A(t)$ with $A(0)$ decays exponentially over time, with a rate determined by the friction coefficient γ. As previously noted, this indicates that correlations between the initial value $A(0)$ and the value at a later time $A(t)$ diminish over time due to dissipation. Moreover, the covariance result does not depend on the stochastic force $\xi(t)$ or the external force $F_{\text{ext}}(t)$, provided these are uncorrelated with $A(0)$.

[2] It is not necessary to impose any of these conditions. By working with autocorrelation, it is possible to handle both systems that are initially in equilibrium, $\langle A(0)\rangle = 0$, and systems that are initially out of equilibrium.

If $\langle A(0)\rangle = 0$, based on the ensemble average of Eq. (2.5), it follows that $\langle A(t)\rangle$ is determined only by the contribution of the external force $F_{\text{ext}}(t)$. On the other hand, the covariance is written as

$$\text{Cov}[A(t), A(0)] = \langle A^2(0)\rangle e^{-\gamma t}$$

with $\sigma_A^2(0) = \langle A^2(0)\rangle$, reestablishing the behavior of Eq. (2.9), i.e., $\text{Cov}[A(t), A(0)] = C_A(t)$.

This result indicates that after a sufficiently long time $t \gg 1/\gamma$, the system will lose any correlation with its initial conditions. In other words, the conditions of mixing and ergodicity are fulfilled [20]. Furthermore, since the temporal evolution of the momentum correlation exhibits exponential decay, it proves that the process in question is Gaussian-Markovian, in accordance with Doob's theorem [71].

Another significant result is the Fluctuation-Dissipation Theorem. Here, we derive it based on the variance of $A(t)$, assuming the external force is deterministic or independent of $A(0)$. Expanding Eq. (2.5) squared and taking the ensemble average, we obtain

$$\begin{aligned}\langle A^2(t)\rangle = \langle A^2(0)\rangle e^{-2\gamma t} + 2\langle A(0)\rangle e^{-\gamma t}\int_0^t e^{-\gamma(t-t')}F_{\text{ext}}(t')dt' \\ + D_T\int_0^t e^{-2\gamma(t-t')}dt' + \left[\int_0^t e^{-\gamma(t-t')}F_{\text{ext}}(t')dt'\right]^2.\end{aligned} \tag{2.14}$$

To this end, we consider conditions (2.2), (2.4), (2.3), and that $\langle \xi(t')F_{\text{ext}}(t'')\rangle = \langle F_{\text{ext}}(t)\xi(t')\rangle = 0$, since $\xi(t)$ is independent of $F_{\text{ext}}(t)$.

From Eq. (2.11), we have

$$\begin{aligned}\langle A(t)\rangle^2 &= \langle A(0)\rangle^2 e^{-2\gamma t} + 2\langle A(0)\rangle e^{-\gamma t}\int_0^t e^{-\gamma(t-t')}F_{\text{ext}}(t')dt' \\ &\quad + \left[\int_0^t e^{-\gamma(t-t')}F_{\text{ext}}(t')dt'\right]^2.\end{aligned} \tag{2.15}$$

Substituting (2.14) and (2.15) into the definition of variance, Eq. (2.13),

$$\begin{aligned}\sigma_A^2(t) &= \sigma_A^2(0)e^{-2\gamma t} + D_T\int_0^t e^{-2\gamma(t-t')}dt'. \\ &= \sigma_A^2(0)e^{-2\gamma t} + \frac{D_T}{2\gamma}\left(1 - e^{-2\gamma t}\right).\end{aligned} \tag{2.16}$$

The first term on the right-hand side of this expression represents the exponential decay of the initial variance due to dissipation. The second term, in contrast, reflects the increase in variance over time due to the noise $\xi(t)$.

In the long-time limit ($t \to \infty$), associated with thermodynamic equilibrium,

$$\sigma_{A,\text{ eq.}}^2 = \lim_{t\to\infty}\sigma_A^2(t) = \frac{D_T}{2\gamma}, \tag{2.17}$$

the variance $\sigma_A^2(t)$ reaches a stationary value that depends on the noise intensity D_T and the friction coefficient γ. To determine the value of D_T, we can relate the stationary

variance $\lim_{t\to\infty}\sigma_A^2(t)$ to the system's absolute temperature T, using the Equipartition Theorem.

At sufficiently long times, i.e., when $t \gg 1/\gamma$ (which mathematically corresponds to the limit $t \to \infty$), the value of $\langle A^2(t)\rangle$ stabilizes and is directly related to the system's kinetic temperature. At thermal equilibrium reached at $t \to \infty$, the average kinetic energy per quadratic degree of freedom is expressed as:

$$\left\langle \frac{1}{2}mv^2(t) \right\rangle = \frac{1}{2}k_B T,$$

where k_B is Boltzmann's constant.

Considering $A(t) = mv(t)$, which implies $\langle A(t)\rangle = m\langle v(t)\rangle$ and $\langle A^2(t)\rangle = m^2\langle v^2(t)\rangle$, we can express the variance of $A(t)$ in terms of kinetic energy. At thermal equilibrium, based on Eq. (2.11) and in the absence of an external force, the average particle velocity is zero due to the lack of preferential motion.

The same result is obtained depending on the behavior of $F_{\text{ext}}(t)$ at long times. Consider the last term on the right-hand side of Eq. (2.11):

$$I(t) = \int_0^t e^{-\gamma(t-t')} F_{\text{ext}}(t')\, dt'. \tag{2.18}$$

Using the Final Value Theorem of the Laplace Transform[3] [73] in the limit as $t \to \infty$,

$$\lim_{t\to\infty} I(t) = \lim_{z\to 0}\left(\frac{z\tilde{F}_{\text{ext}}(z)}{z+\gamma}\right). \tag{2.19}$$

This result indicates that we need to understand the behavior of $\tilde{F}_{\text{ext}}(z)$ as $z \to 0$ to predict whether or not there is a preferential motion. As an example:

1. If the external force is constant, the accumulated effect is counterbalanced by dissipation, leading to a finite value of $I(t)$; thus, there will be a preferential average velocity in the system.

2. If the external force decays exponentially, losing its effect in the long term, the system dissipates this influence, resulting in no accumulated effect in the long-time limit, i.e., $\langle v(t \to \infty)\rangle \to 0$.

3. For an oscillating force, e.g., $F_{\text{ext}}(t) = F_0\cos(\omega t)$, the Laplace transform results in

$$\tilde{F}_{\text{ext}}(z) = \frac{F_0 z}{z^2+\omega^2},$$

[3] The Final Value Theorem of the Laplace Transform states that if $f(t)$ is a real, continuous, and absolutely integrable function on $[0,\infty)$ whose Laplace transform $\mathcal{L}\{f(t)\}$ exists for z near zero, and if $f(t)$ has a finite limit as $t \to \infty$, then [72]:

$$\lim_{t\to\infty} f(t) = \lim_{z\to 0} z\mathcal{L}\{f(t)\}.$$

with $I(t \to \infty) \to 0$, meaning it also does not contribute to a permanent displacement in the system due to dissipation and the time average of the oscillations.

Therefore, for cases where Eq. (2.11) is null for long times,

$$\sigma^2_{A,\,\text{eq.}} = \lim_{t\to\infty} \left\langle A^2(t) \right\rangle = mk_BT.$$

Comparing this to Eq. (2.17) in the limit as $t \to \infty$, we have

$$D_T = 2m\gamma k_BT. \tag{2.20}$$

The fluctuation-dissipation theorem can then be written, based on Eq. (2.3), as

$$\langle \xi(t)\xi(t') \rangle = 2m\gamma k_BT\delta(t-t'). \tag{2.21}$$

This result is crucial for understanding stochastic processes in physical systems, as it connects microscopic properties (thermal fluctuations) to macroscopic observables (dissipation and temperature).

We can establish a complementary analysis regarding the impacts of the external force. As discussed earlier, assuming the validity of the Energy Equipartition Theorem, $\langle A^2(t \to \infty) \rangle = mk_BT$, which leads to

$$\lim_{t\to\infty} \langle A^2(t) \rangle = \sigma^2_{A,\,\text{eq.}} + \lim_{t\to\infty} \langle A(t) \rangle^2 = mk_BT, \tag{2.22}$$

so that, considering Eq. (2.17),

$$D_T = 2m\gamma k_BT - \Lambda_T, \tag{2.23}$$

where $\Lambda_T = 2\gamma \lim_{t\to\infty} \langle A(t) \rangle^2$. Consequently, the fluctuation-dissipation theorem must be corrected as follows:

$$\langle \xi(t)\xi(t') \rangle = (2m\gamma k_BT - \Lambda_T)\,\delta(t-t'). \tag{2.24}$$

Considering Eq. (2.15), note that in the limit $t \to \infty$, the first term on the right-hand side vanishes. In the second term, the exponential factor $e^{-\gamma t}$ decays to zero for long times. However, the integral $I(t)$, Eq. (2.18), as previously discussed, depends on the form of $F_{\text{ext}}(t)$. To analyze the asymptotic behavior, we assume that $F_{\text{ext}}(t)$ is bounded or does not grow faster than an exponential of rate $\tau < \gamma$. In this case, $I(t)$ remains finite or grows more slowly than $e^{\gamma t}$. Therefore, $\lim_{t\to\infty} e^{-\gamma t} I(t) = 0$. Finally, the third term depends critically on the asymptotic behavior of $F_{\text{ext}}(t)$ as $t \to \infty$.

Again, from the Final Value Theorem of the Laplace Transform, we analyze the asymptotic behaviors of $F_{\text{ext}}(t)$ and its Laplace transform $\tilde{F}_{\text{ext}}(z)$ to determine whether $I^2(t)$ tends to zero, a constant value, or diverges. Assuming

$$\lim_{z\to 0} \tilde{F}_{\text{ext}}(z) \sim z^{\beta_F} \tag{2.25}$$

in the asymptotic behavior, since $I^2(t) = I(t) \cdot I(t)$, the Algebraic Limit Theorem[4] allows us to rewrite Eq. (2.19) as

$$\lim_{t\to\infty} I^2(t) = \left(\lim_{t\to\infty} I(t)\right)^2 = \left(\frac{1}{\gamma}\lim_{z\to 0} z\tilde{F}_{\text{ext}}(z)\right)^2. \tag{2.26}$$

Hence, the asymptotic behavior of $I^2(t)$ directly depends on the behavior of $z\tilde{F}_{\text{ext}}(z)$ as $z \to 0$.

Suppose that as $z \to 0$, the Laplace transform of $F_{\text{ext}}(t)$ behaves asymptotically as $\tilde{F}_{\text{ext}}(z) \sim kz^{\beta_F}$, where k is a real constant and β_F is the exponent characterizing the asymptotic behavior. Substituting into Eq. (2.26),

$$\lim_{t\to\infty} I^2(t) = \left[\frac{1}{\gamma}\lim_{z\to 0} z(kz^{\beta_F})\right]^2 = \left(\frac{k}{\gamma}\lim_{z\to 0} z^{\beta_F+1}\right)^2. \tag{2.27}$$

If $\beta_F + 1 > 0$ (i.e., $\beta_F > -1$), as $z \to 0$, $z^{\beta_F+1} \to 0$. Thus, $\lim_{t\to\infty} I^2(t) = 0$, and the fluctuation-dissipation theorem for normal diffusion, Eq. (2.21), is satisfied. This behavior is observed for functions such as exponentially decaying ones, e.g., $F_{\text{ext}}(t) = F_0 e^{-\lambda t}$ with $\lambda > 0$ and F_0 constant, potentially decaying functions, e.g., $F_{\text{ext}}(t) = F_0/(1+t)^a$ with $a > 0$, or bounded oscillatory functions, e.g., $F_{\text{ext}}(t) = F_0 \cos(\omega t)$.

If $\beta_F + 1 = 0$ (i.e., $\beta_F = -1$), we have $z^{\beta_F+1} = 1$. Then, $\lim_{t\to\infty} I^2(t) = (k/\gamma)^2$. In this case, the usual fluctuation-dissipation theorem, Eq. (2.21), does not hold, and the correction Λ_T becomes necessary. This is the case for $F_{\text{ext}}(t) = F_0$, where F_0 is constant.

Finally, if $\beta_F + 1 < 0$ (i.e., $\beta_F < -1$), $z^{\beta_F+1} \to \infty$, because the exponent is negative. Hence, $\lim_{t\to\infty} I^2(t) \to \infty$. With the divergence of $I^2(t)$ as $t \to \infty$, it is observed that the second term on the right-hand side of Eq. (2.15) can also diverge, which may reverberate in the value of $\langle A^2(t)\rangle$, Eq. (2.14), such that neither a fluctuation-dissipation relation nor the Algebraic Limit Theorem can be defined.

2.3 Generalized Langevin Equation

Until now, we have only considered interactions that depend on the generalized positions and momenta of the immediately preceding instant, characterizing Markovian processes, which lack memory. However, it is possible to extend this study based on the Langevin equation to systems where interactions possess memory [8, 9]. In these cases, the

[4] Algebraic Limit Theorem: Let $f(x)$ and $g(x)$ be functions defined in an interval containing the point p, except possibly at p itself, and suppose the limits $\lim_{x\to p} f(x)$ and $\lim_{x\to p} g(x)$ exist and are finite. Then, the limit of the product of the functions $f(x)$ and $g(x)$ equals the product of the individual limits:

$$\lim_{x\to p}(f(x)\cdot g(x)) = \left(\lim_{x\to p} f(x)\right)\cdot\left(\lim_{x\to p} g(x)\right).$$

correlations exhibit behaviors different from those observed in Sections 2.1 and 2.2, and the temporal evolution may depend on the system's initial conditions. Such processes are termed non-Markovian and are frequently used to describe anomalous diffusion [74, 10, 65].

Starting from the friction term of the normal Langevin equation, Eq. (2.1), we can generalize it as

$$\gamma A(t) \to \int_0^t dt' \Gamma(t-t') A(t'), \tag{2.28}$$

where the memory function $\Gamma(t-t')$ retains information about previous moments [74] and/or the initial instant. Thus, the Generalized Langevin Equation is defined as [8, 9]

$$\frac{dA}{dt} = -\int_0^t \Gamma(t-t') A(t') dt' + \xi(t) + F_{\text{ext}}(t), \tag{2.29}$$

where $\xi(t)$ is the stochastic noise term and $F_{\text{ext}}(t)$ represents an applied external force.

Note that this is a generalization of the Normal Langevin Equation, Eq. (2.1). In the specific case where $\Gamma(t-t') = 2\gamma\delta(t-t')$, the filtering property of the Dirac delta function allows only the term $-\gamma A(t)$ to be recovered. This is expected, as the memory function would be correlated only with the instant t, carrying no information about previous times, characteristic of a Markovian process.

The temporal dynamics of this type of non-Markovian process can be determined using the Laplace transform of the Generalized Langevin Equation, yielding

$$\tilde{A}(z) = A(0)\tilde{R}(z) + \tilde{\xi}(z)\tilde{R}(z) + \tilde{F}_{\text{ext}}(z)\tilde{R}(z), \tag{2.30}$$

where the relaxation function $\tilde{R}(z)$ is defined as [66]

$$\tilde{R}(z) = \frac{1}{z + \tilde{\Gamma}(z)}. \tag{2.31}$$

The inverse Laplace transform of the expression for $\tilde{A}(z)$ provides the temporal evolution of the variable $A(t)$,

$$A(t) = A(0)R(t) + \int_0^t dt' R(t-t') \left[\xi(t') + F_{\text{ext}}(t')\right], \tag{2.32}$$

where $R(t)$ is the inverse Laplace transform of $\tilde{R}(z)$.

In the Generalized Langevin Equation, Eq. (2.29), the noise term $\xi(t)$ is a stochastic process whose autocorrelation function $C_\xi(t)$, unlike white noise, is characterized by temporal correlations. Mathematically, the colored noise $\xi(t)$ satisfies the zero-mean relation,

$$\langle \xi(t) \rangle = 0, \tag{2.33}$$

and the autocorrelation relation,

$$C_\xi(t-t') = \langle \xi(t)\xi(t') \rangle = \phi(t-t'), \tag{2.34}$$

where $\phi(t-t')$ is the autocorrelation function depending on the time difference $t-t'$. This noise with temporal correlations is known as "colored" noise [8, 65, 7, 75]. Several types of colored noises can be cited [75]:

1. Ornstein-Uhlenbeck noise, characterized by exponentially decaying correlation, where
$$\phi(t) = \frac{D}{\tau} e^{-\frac{|t|}{\tau}},$$
where D_T is the noise intensity and τ is the correlation time.

2. $1/f$ noise, which has a power spectral density $S(\nu)$ that decays inversely with frequency ν, i.e.,
$$S(\nu) \propto \frac{1}{\nu^{\alpha}}, \quad \text{with } 0 < \alpha \leq 2.$$

3. Correlated Gaussian noise, where $\phi(t)$ can take other functional forms, such as Bessel functions or modulated exponentials.

Colored noise is essential for describing systems where Markovian approximations (memoryless) are not suitable. In this work, we consider Gaussian noise that, in addition to satisfying conditions (2.33) and (2.34), also meets the causal relationship

$$\langle A(0)\xi(t)\rangle = 0. \tag{2.35}$$

Now, moving the contribution of the external force term, F_{ext}, to the left-hand side of Eq. (2.32), we define a new characteristic variable:

$$A^{\dagger}(t) = A(t) - \int_0^t dt' R(t-t') F_{\text{ext}}(t'), \tag{2.36}$$

which satisfies the equality

$$A^{\dagger}(t) = A^{\dagger}(0)R(t) + \int_0^t R(t-t')\xi(t')dt', \tag{2.37}$$

where, by construction, $A^{\dagger}(0) = A(0)$.

On the other hand, since both Eq. (2.37) and Eq. (2.32) are formally similar, we infer that, just as Eq. (2.32) is the solution to Eq. (2.29), Eq. (2.37) must be the solution to

$$\frac{dA^{\dagger}(t)}{dt} = -\int_0^t \Gamma(t-t')A^{\dagger}(t')dt' + \xi(t), \tag{2.38}$$

corresponding to the Generalized Langevin Equation in the absence of an external force. Furthermore, given the properties of $\xi(t)$ mentioned in the context of Eq. (2.29), we conclude that Eq. (2.38) describes a stationary Gaussian process.

Multiplying Eq. (2.38) by $A^{\dagger}(0)$, taking the ensemble average, and using Eq. (2.41), we obtain

$$\frac{d}{dt}R(t) = -\int_0^t \Gamma(t-t')R(t')\,dt'. \tag{2.39}$$

Taking the ensemble average of $A^\dagger(t)$ from Eq. (2.37), we find

$$\langle A^\dagger(t)\rangle = \langle A^\dagger(0)\rangle R(t). \tag{2.40}$$

Multiplying Eq. (2.37) by $A^\dagger(0)$, taking the ensemble average, considering condition (2.35), and dividing by $\langle A^{\dagger 2}(0)\rangle$, we obtain

$$R(t) = \frac{C_{A^\dagger}(t)}{C_{A^\dagger}(0)} = \frac{\left\langle A^\dagger(t)A^\dagger(0)\right\rangle}{\langle A^{\dagger 2}(0)\rangle}, \tag{2.41}$$

which expresses the response function $R(t)$ defined above in terms of the two-time correlation of the variable $A^\dagger$ in the absence of an external force.

Similarly, multiplying Eq. (2.32) by $A(0)$, taking the ensemble average, and dividing by $\langle A^2(0)\rangle$, we find

$$R_0(t) = \frac{\langle A(t)A(0)\rangle}{\langle A^2(0)\rangle} = R(t) + \epsilon \int_0^t dt' R(t-t') F_{\rm ext}(t'), \tag{2.42}$$

where $\epsilon = \langle A(0)\rangle / \langle A^2(0)\rangle$.

As we did in Section 2.2, expanding Eq. (2.37) squared and calculating the ensemble average, we have

$$\begin{aligned}\left\langle A^{\dagger 2}(t)\right\rangle &= \left\langle A^{\dagger 2}(0)\right\rangle R^2(t) + 2R(t)\int_0^t R(t-t')\left\langle A(0)\xi(t')\right\rangle dt' + \\ &\quad + \int_0^t\int_0^t R(t-t')R(t-t'')\left\langle \xi(t')\xi(t'')\right\rangle dt'dt''. \end{aligned}\tag{2.43}$$

Now, let us focus on the last term on the right-hand side of this expression,

$$g(t) = \int_0^t\int_0^t R(t-t')R(t-t'')\left\langle \xi(t')\xi(t'')\right\rangle dt'dt''. \tag{2.44}$$

To apply the principle of time-translation symmetry to $g(t)$, we assume that the noise autocorrelation function $C_\xi(t'-t'')$ is even, allowing us to rewrite Eq. (2.44) as

$$\begin{aligned} g(t) &= \int_0^t R(t')\left[\int_0^t \phi(t'-t'')R(t'')dt''\right]dt' \\ &= \int_0^t R(t')\left[\int_0^{t'} \phi(t'-t'')R(t'')dt''\right]dt' + \int_0^t R(t')\left[\int_{t'}^t \phi(t'-t'')R(t'')dt''\right]dt'. \end{aligned}$$

By inverting the order of integration in the above equation, we obtain

$$\int_0^t R(t')\left[\int_{t'}^t \phi(t'-t'')R(t'')dt''\right]dt' = \int_0^t R(t'')\left[\int_0^{t''} \phi(t'-t'')R(t')dt'\right]dt'',$$

which results in

$$g(t) = 2\int_0^t R(t')\left[\int_0^{t'} \phi(t'-t'')R(t'')dt''\right]dt'.$$

Next, let us assume that the function $\phi(t-t')$ is proportional to the memory function, i.e.,

$$\phi(t-t') = D_T\Gamma(t-t'), \tag{2.45}$$

where the parameter D_T is treated as a proportionality constant, whose value must be determined through appropriate analysis. Using Eq. (2.39), we find

$$\begin{aligned} g(t) &= -2D_T\int_0^t \frac{1}{2}\frac{d\left[R^2(t')\right]}{dt'}dt' \\ &= D_T\left[1-R^2(t)\right]. \end{aligned} \tag{2.46}$$

Note that $R(0)=1$, as indicated by Eq. (2.41).

Finally, substituting Eq. (2.46) into Eq. (2.43) and considering condition (2.35), we arrive at

$$\left\langle A^{\dagger 2}(t)\right\rangle = D_T + \left[\left\langle A^{\dagger 2}(0)\right\rangle - D_T\right]R^2(t). \tag{2.47}$$

2.4 Relaxation Function

First, it is important to note that the long-time behavior is associated with small values of z in the Laplace transform. From the Final Value Theorem [73], we have

$$\lim_{t\to\infty} R(t) = \lim_{z\to 0} z\tilde{R}(z). \tag{2.48}$$

Morgado *et al.* [76] obtained a general relation between the Laplace transform of the memory function $\tilde{\Gamma}(z)$ and the diffusion exponent α:

$$\lim_{z\to 0}\tilde{\Gamma}(z) \approx c_T z^{\alpha-1}, \tag{2.49}$$

where c_T is a positive dimensionless constant. Using Eq. (2.49) in Eq. (2.48), we obtain

$$\lim_{t\to\infty} R(t) = \lim_{z\to 0}\left(1+c_T z^{\alpha-2}\right)^{-1}. \tag{2.50}$$

This expression is zero for all diffusive processes in the interval $0<\alpha<2$. This occurs because, for $\alpha<2$, the exponent $\alpha-2$ is negative, causing $z^{\alpha-2}$ to diverge as $z\to 0$, resulting in $R(t\to\infty)\to 0$. This behavior is typical of equilibrium or near-equilibrium states where the validity of Linear Response Theory is maintained.

On the other hand, this condition does not apply to ballistic motion, when $\alpha=2$. In this case, we have

$$\lim_{t\to\infty} R(t) = \left(1+c_T\right)^{-1}, \tag{2.51}$$

and the autocorrelation function $C_{A^\dagger}(t)$ does not vanish at long times. This means that if the ballistic system is not initially in equilibrium, it will never reach equilibrium, and the

final result of any measurement will depend on the initial conditions [21]. In this situation, the Ergodic Hypothesis is not valid.

However, Khinchin's Theorem remains valid, as the violation of the Ergodic Hypothesis is due to the breakdown of the irreversibility condition, Eq. (2.50), as anticipated by Khinchin [77]. The main consequence of this violation is the presence of a residual current, Eq. (2.40), which drives the system to a preferential momentum (*drift* effect). Nonetheless, this effective current may be very small compared to $\langle A^\dagger(0)\rangle$, and its value, as well as any other measurable property in ballistic diffusion, will depend on the value of c_T.

In other words, the system decays into a metastable state and remains in it indefinitely, even in the absence of an external field. Consequently, the effective kinetic temperature, Eq. (2.59), does not reach the expected value at long times, which would correspond to the thermal reservoir temperature.

Another situation to highlight is the effect of external force on $R(t)$. From Eq. (2.36), we obtain

$$\begin{aligned} R(t) = \frac{C_{A^\dagger}(t)}{C_{A^\dagger}(0)} &= \frac{\langle A(t)A(0)\rangle}{\langle A^2(0)\rangle} - \frac{\langle A(0)\rangle}{\langle A^2(0)\rangle}\int_0^t R(t-t')F_{\text{ext}}(t')dt' \\ &= R_0(t) - \epsilon\int_0^t R(t-t')F_{\text{ext}}(t')dt', \end{aligned} \tag{2.52}$$

where $R_0(t) = \langle A(t)A(0)\rangle/\langle A^2(0)\rangle$ is the relaxation function in the presence of an external force, and $\epsilon = \langle A(0)\rangle/\langle A^2(0)\rangle$, where we consider $\langle A^\dagger(0)\rangle = \langle A(0)\rangle$. Note that in cases where the external force is zero or $\langle A(0)\rangle = 0$, $R(t) = R_0(t)$.

Otherwise, for $\langle A(0)\rangle \neq 0$ and under the effect of an external force, let us apply the Laplace transform to Eq. (2.52). Thus, we obtain

$$\tilde{R}_0(z) = \tilde{R}(z) + \epsilon\tilde{R}(z)\tilde{F}_{\text{ext}}(z). \tag{2.53}$$

Rearranging this expression, we can write

$$\tilde{R}_0(z) = \left[1 + \epsilon\tilde{F}_{\text{ext}}(z)\right]\tilde{R}(z). \tag{2.54}$$

From Eq. (2.31), we have

$$\tilde{R}_0(z) = \frac{1 + \epsilon\tilde{F}_{\text{ext}}(z)}{z + \tilde{\Gamma}(z)}. \tag{2.55}$$

Let us analyze the asymptotic behavior of $R_0(t)$ for $t \to \infty$, using the Final Value Theorem of the Laplace transform. We aim to express $z\tilde{R}_0(z)$ in terms of the asymptotic forms of $\tilde{F}_{\text{ext}}(z)$, Eq. (2.25), and $\tilde{\Gamma}(z)$, Eq. (2.49), which are, respectively:

$$\tilde{F}_{\text{ext}}(z) \sim kz^{\beta_F} \quad \text{and} \quad \tilde{\Gamma}(z) \sim cz^{\alpha-1},$$

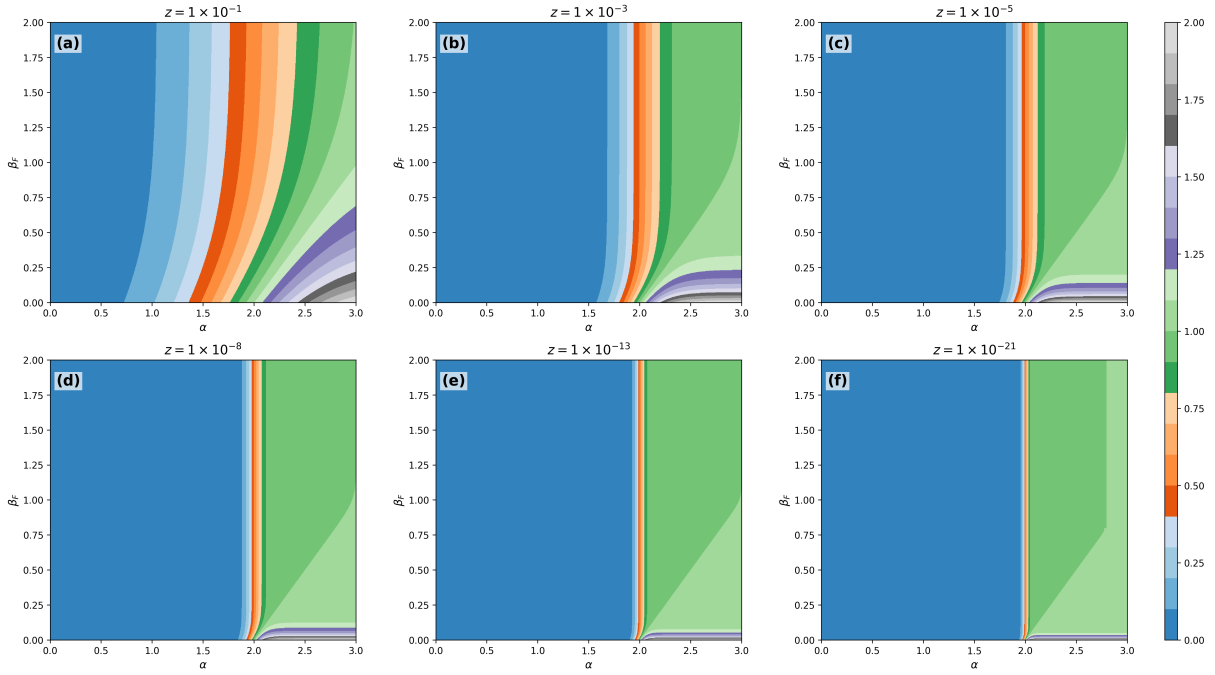

Figure 1. Relaxation function $R_0(t)$ in the plane of the diffusion exponent α and the asymptotic exponent of the external force β_F, based on the behavior of $z\tilde{R}_0(z)$ in the Laplace space. **(a)**-**(f)** $zR_0(z)$ for specific values of z, varying from: **(a)** $z = 1 \times 10^{-1}$, transient regime, to **(f)** $z = 1 \times 10^{-21}$, steady-state regime.

where k and c_T are positive constants. As previously discussed, β_F and α are exponents characterizing the asymptotic behavior.

Since we are interested in the asymptotic behavior as $z \to 0$, we can substitute the functions with their dominant-order approximations [78]. This means that instead of considering the full expression for $\tilde{F}_{\text{ext}}(z)$ and $\tilde{\Gamma}(z)$, we use only the terms that contribute most as $z \to 0$. In other words, higher-order terms (with larger powers of z) become insignificant compared to the dominant-order terms. Thus, substituting $\tilde{F}_{\text{ext}}(z)$ and $\tilde{\Gamma}(z)$ with their asymptotic forms in Eq. (2.55),

$$z\tilde{R}_0(z) \sim \frac{1 + \epsilon k z^{\beta_F}}{1 + c_T z^{\alpha-2}}. \tag{2.56}$$

Figure 1 illustrates the asymptotic behavior of $R_0(t)$ for long times as a function of the parameters α and β_F, considering fixed values of z, obtained from Eq. (2.56). In this analysis, the parameters $\epsilon = k = c_T = 1$ were used. Each subplot corresponds to a color map of $z\tilde{R}_0(z)$ in Laplace space, assuming the relationship for asymptotic behavior $t \to \lambda/z$, where the scaling factor is given by

$$\lambda = 1 - \lim_{t\to\infty} t\frac{d\ln[f(t)]}{dt},$$

with $f(t) = \lambda + t\tilde{\Gamma}(\lambda/t)$ [79], which relates the time t and Laplace z spaces.

The transient regime, characterized by times shorter than the characteristic relaxation time, is represented in Fig. 1**a**, with $z = 1 \times 10^{-1}$. In this regime, results are less precise due to the disregard of other dominant orders for the memory function and external force. Precision improves as z decreases, as shown in Fig. 1**f**, where $z = 1 \times 10^{-21}$. This regime, called steady-state due to stationarity, features more defined contours, aligning with the theoretical behaviors analyzed later and suggesting a phase transition between diffusive and hydrodynamic processes [80, 81, 82].

In the adopted color scale, the correspondence to $\lim_{t\to 0} R_0(t) = 0$ (dark blue) indicates that the system loses "memory" of the initial conditions and thermalizes with the thermal bath (see Eq. (2.59)), satisfying Khinchin's Theorem [77], the Fluctuation-Dissipation Theorem (Eq. (2.34)) [20], and the Ergodic Hypothesis [18], with the probability density function converging to a Gaussian distribution [21]. This regime prevails for situations where $\alpha < 2$. In the range where $0 < \lim_{t\to\infty} R_0(t) < 1$, violating the aforementioned theorems and the ergodic hypothesis, the probability density function depends on the system's initial conditions. A narrow range around $\alpha = 2$ for $\beta_F > 0$ is observed, characterizing a phase transition from the diffusive to the hydrodynamic regime. Situations where $\lim_{t\to\infty} R_0(t) > 1$ indicate that the system is highly correlated under the dominance of the external force.

We include values referring to the hyperballistic regime ($\alpha > 2$), extensively studied in the literature involving quantum or classical particles in random potentials [83, 84], with behaviors similar to those described by the Generalized Langevin Equation and optical experiments [85, 86], where the spatial coordinate in the direction of light plays the role of the temporal coordinate.

To understand the behavior of $zR_0(z)$ as $z \to 0$, it is essential to consider the terms on the right-hand side of Eq. (2.56). The first term in the numerator is constant, equal to 1, and remains unchanged regardless of the values of α and β_F. The second term, $\epsilon k z^{\beta_F}$, depends directly on the value of β_F.

When $\beta_F > 0$, z^{β_F} tends to zero, and the asymptotic behavior becomes independent of the external force, relying solely on the diffusion exponent α: 1. If $\alpha > 2$, $R(t \to \infty) \to 1$; 2. if $\alpha = 2$, $R(t \to \infty) \to 1/(1 + c_T)$; and 3. if $\alpha < 2$, $R(t \to \infty) \to 0$.

When $\beta_F = 0$, the asymptotic behavior of $R_0(t)$ for long times will depend on $(1 + \epsilon k)/(1 + c_T z^{\alpha-2})$. 1. If $\alpha > 2$, $R(t \to \infty) \to 1 + \epsilon k$; 2. if $\alpha = 2$, $R(t \to \infty) \to (1 + \epsilon k)/(1 + c_T)$; and 3. if $\alpha < 2$, $R(t \to \infty) \to 0$.

When $\beta_F < 0$, z^{β_F} diverges as $z \to 0$. Therefore, $\epsilon k z^{\beta_F}$ becomes the dominant term in the numerator. 1. When $\alpha > 2$, we obtain

$$z\tilde{R}_0(z) \sim \epsilon k z^{\beta_F}.$$

Since $\beta_F < 0$, $z^{\beta_F} \to \infty$, so $z\tilde{R}(z) \to \infty$, and the external force dominates over diffusion

effects. 2. When $\alpha = 2$,

$$z\tilde{R}(z) \sim \frac{\epsilon k z^{\beta_F}}{1 + c_T}.$$

Thus, $z^{\beta_F} \to \infty$, leading to $z\tilde{R}_0(z) \to \infty$, as in the previous case. 3. For $\alpha < 2$,

$$z\tilde{R}(z) \sim \frac{\epsilon k z^{\beta_F}}{c_T z^{\alpha-2}} = \frac{\epsilon k}{c_T} z^{\beta_F-(\alpha-2)} = \frac{\epsilon k}{c_T} z^{\beta_F-\alpha+2}.$$

3.1. If $\beta_F - \alpha + 2 < 0$: $z^{\beta_F-\alpha+2} \to \infty$, then $z\tilde{R}_0(z) \to \infty$. In this case, the system does not reach thermal equilibrium, as $R_0(t)$ grows indefinitely, indicating a tendency toward persistent preferential motion. If $\beta_F - \alpha + 2 = 0$: $z^{\beta_F-\alpha+2} = 1$, then $z\tilde{R}_0(z) \approx \frac{\epsilon k}{c_T}$. Thus, the system reaches a stable equilibrium state where the influence of external force and dissipation balance out. Finally, if $\beta_F - \alpha + 2 > 0$: $z^{\beta_F-\alpha+2} \to 0$, then $z\tilde{R}_0(z) \to 0$. In this case, the system completely dissipates external influences, returning to thermal equilibrium without preferential motion.

Conditions	**Dominant Term**	**Asymptotic** $zR(z)$
$\beta_F > 0$ and $\alpha > 2$	1	1
$\beta_F > 0$ and $\alpha = 2$	$\frac{1}{1+c_T}$	$\frac{1}{1+c_T}$
$\beta_F > 0$ and $\alpha < 2$	$\frac{1}{c_T z^{\alpha-2}}$	0
$\beta_F = 0$ and $\alpha > 2$	$1 + \epsilon k$	$1 + \epsilon k$
$\beta_F = 0$ and $\alpha = 2$	$\frac{1+\epsilon k}{1+c_T}$	$\frac{1+\epsilon k}{1+c_T}$
$\beta_F = 0$ and $\alpha < 2$	$\frac{1+\epsilon k}{c_T z^{\alpha-2}}$	0
$\beta_F < 0$, $\alpha \geq 2$	$\frac{1}{z^{\lvert\beta_F\rvert}}$	∞
$\beta_F < 0$, $0 \leq \alpha < 2$	$\frac{\epsilon k}{c_T} z^{\beta_F-\alpha+2}$	$\begin{cases} 0, & \text{if } \eta > 0, \\ \frac{\epsilon k}{c_T}, & \text{if } \eta = 0, \\ \infty, & \text{if } \eta < 0. \end{cases}$

Table 1. Asymptotic behavior of $R(t)$ for long times derived from the Final Value Theorem of Laplace Transform with $\eta = \beta_F - \alpha + 2$.

Table 1 summarizes the asymptotic behavior of $zR(z)$ for different combinations of α and β_F. As $z \to 0$, terms with negative or smaller exponents tend to grow if β_F or $\alpha - 2$ are negative, or vanish if the exponents are positive. The results demonstrate how the parameters α and β_F significantly influence the asymptotic behavior of $zR(z)$. For $\beta_F > 0$ and $\alpha > 2$, $zR(z)$ approaches 1, indicating that contributions from $F_{\text{ext}}(t)$ direct the system towards a regime where the initial conditions are fully preserved, resulting in a net balance between the external force and dissipation. In the case of $\beta_F > 0$ and $\alpha = 2$, $zR(z)$ converges to $(1 + c_T)^{-1}$, reflecting a constant contribution from the memory function, such that the effect of the external force does not impact the system's relaxation process. This situation is similar to the ballistic case without an external force [18]. For $\beta_F > 0$ and $\alpha < 2$, $zR(z)$ tends to zero proportional to $z^{2-\alpha}$. This indicates that the memory function dominates the denominator's behavior, causing $R(t)$ to decrease further as t increases. This behavior is characteristic of regimes where dissipation plays a dominant role in the system.

In the regime of $\beta_F = 0$ and $\alpha < 2$, diffusive behavior dominates, and fluctuation-dissipation relations are preserved. In the ballistic regime, $\alpha = 2$, $zR(z)$ converges to $(1 + \epsilon k)/(1 + c)$, showing that both $F_{\text{ext}}(t)$ and $\Gamma(t)$ contribute consistently to the denominator. This adjusts $zR(z)$ according to the parameters k and c, representing a critical point where a phase transition from the diffusive to the hydrodynamic regime is observed. For $\beta_F = 0$ and $\alpha > 2$, the effects of the external force dominate the system's behavior, and no relation presented here is satisfied.

Another interesting regime occurs for $\beta_F < 0$. In the hyperballistic and ballistic cases, $\alpha \geq 2$, the drift effect induced by the external force dominates the system's evolution, such that none of the results presented here can be applied. Conversely, for $\alpha < 2$, the parameter $\eta = \beta_F - \alpha + 2$ enables phase transitions between diffusive regimes satisfying Khinchin's Theorem, hydrodynamic processes, and scenarios dominated by external force tendencies. Figure 2 shows the phase transition from the diffusive to the non-diffusive regime based on the behavior of $z\tilde{R}(z)$ for $z = 1.0 \times 10^{-100}$, with $\epsilon = 1$, $k = 0.2$, and $c = 0.4$. The transition is well-defined for $\eta = 0$ for values of $\beta_F < 0$. The white color represents $z\tilde{R}(z) \to \infty$. The dashed horizontal line at $\beta_F = 0$ serves as a guide for the transition to $\beta_F > 0$. For values of $\beta_F \geq 0$, note that η still exhibits a discrete influence.

It should be noted, however, that depending on the values of the parameters c, ϵ, and k, compared to the observed time scale, variations in the location of the phase transition may occur, representing a balance among the different influences in the system.

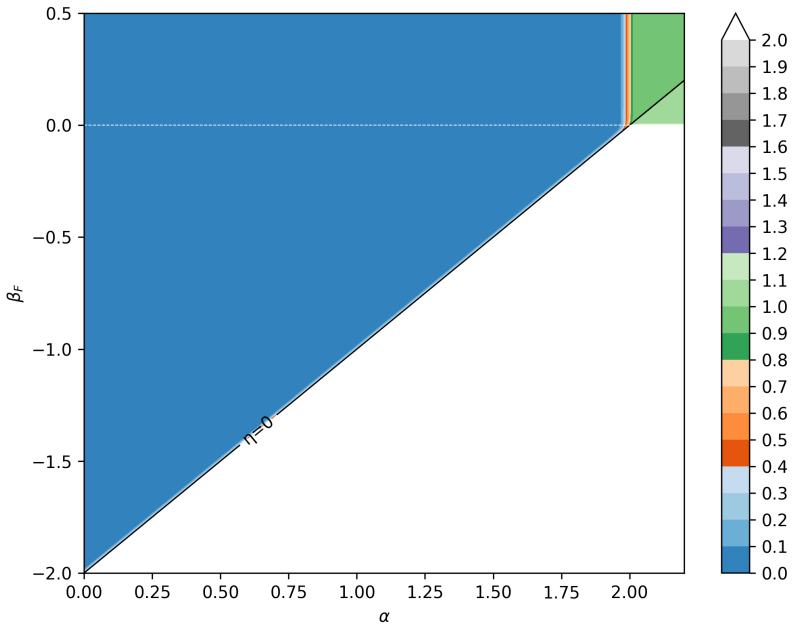

Figure 2. Asymptotic behavior of the relaxation function $R(t)$ in terms of the parameters α and β_F. Fixed values of $\alpha = 2$, $\beta_F < 0$, $z = 1 \times 10^{-100}$, $\epsilon = 1$, $k = 0.2$, and $c = 0.4$ were considered.

2.5 Evolution of the System's Temperature from the Relaxation Function

In the kinetic theory of gases, temperature is directly related to the average kinetic energy of particles. Consequently, analyzing $\langle A^{\dagger 2}(t)\rangle$ provides a direct way to correlate the temperature of a gas with its dispersion in the absence of external forces. For each degree of freedom, $\left\langle A^{\dagger 2}(t)\right\rangle$, derived from Eq. (2.37), can be associated with mk_BT. The physical significance of the constant D_T, formulated from $\phi(t)$, as per Eq. (2.45), arises from the assumption that the system, while progressing towards thermal equilibrium with the heat reservoir over sufficiently long periods, satisfies $R(t \to \infty) \to 0$ [77]. Analogous to the kinetic theory of gases, as discussed in Section 2.2, we associate $\left\langle A^{\dagger 2}(t)\right\rangle$ with an effective kinetic temperature equivalent to $mk_BT_{\text{ef.}}$. Similarly, we adopt the system's initial temperature $\left\langle A^{\dagger 2}(0)\right\rangle = mk_BT_0$ as a reference. Thus, Eq. (2.47) can be rewritten as

$$T_{\text{ef.}}(t) = \frac{D_T}{mk_B} + \left[T_0 - \frac{D_T}{mk_B}\right] R^2(t). \tag{2.57}$$

When Khinchin's theorem is satisfied, such that $\lim_{t\to\infty} R(t) = 0$, we have $\lim_{t\to\infty} \left\langle A^{\dagger 2}(t)\right\rangle \to mk_BT_R$, where T_R is the thermal reservoir temperature. Consequently,

$$D_T = mk_BT_R. \tag{2.58}$$

This term naturally arises in the asymptotic time limit, $t \to \infty$, where the relaxation function $R(t)$ approaches zero, and the thermal fluctuations of the variable $A^{\dagger}$ attain a stationary form determined by the reservoir temperature. Therefore, the fluctuation can be expressed as a function of time, considering that the temperature evolves from an initial condition T_0 to T_R, the equilibrium temperature. This leads to the expression,

$$T_{\text{ef.}}(t) = T_R + [T_0 - T_R]\, R^2(t), \tag{2.59}$$

This equation describes the relaxation of temperature over time, starting from an initial temperature T_0 and converging to T_R, modulated by the relaxation function $R(t)$. The behavior of $R^2(t)$ is crucial for understanding the relaxation rate and how the system transitions from the initial regime to thermal equilibrium.

In the presence of a time-dependent external force, starting from Eq. (2.32) instead of Eq. (2.37), we calculate the ensemble average of the momentum, and using condition (2.33), we obtain

$$\langle A(t)\rangle = \langle A(0)\rangle R(t) + \int_0^t R(t-t')F_{ext}(x,t')dt'. \tag{2.60}$$

The asymptotic limit for long times of $\langle A(t)\rangle$ can be computed using the Final Value Theorem of the Laplace Transform, such that

$$\lim_{t\to\infty}\langle A(t)\rangle = \lim_{z\to 0} z\left[\langle A(0)\rangle + \tilde{F}_{\text{ext.}}(z)\right]\tilde{R}(z), \tag{2.61}$$

which, depending on the behavior of the Laplace transforms of $R(t)$ and $F_{\text{ext}}(t)$, may exhibit a drift effect.

To compute $\langle A^2(t)\rangle$, starting from Eq. (2.32), we obtain

$$\begin{aligned}\langle A^2(t)\rangle &= \langle A^2(0)\rangle R^2(t) + 2\langle A(0)\rangle R(t)\int_0^t R(t-t')F_{\text{ext}}(t')dt' + \\ &\quad + D_T\left[1 - R^2(t)\right] + \left[\int_0^t R(t-t')F_{\text{ext}}(t')dt'\right]^2.\end{aligned} \tag{2.62}$$

Thus, using the property of the Algebraic Limit Theorem,

$$\begin{aligned}\lim_{t\to\infty}\langle A^2(t)\rangle &= \langle A^2(0)\rangle\left[\lim_{t\to\infty}R(t)\right]^2 + \\ &\quad + 2\langle A(0)\rangle\left[\lim_{t\to\infty}R(t)\right]\cdot\left[\lim_{t\to\infty}\int_0^t R(t-t')F_{\text{ext}}(t')dt'\right] + \\ &\quad + D_T\left\{1 - \left[\lim_{t\to\infty}R(t)\right]^2\right\} + \left[\lim_{t\to\infty}\int_0^t R(t-t')F_{\text{ext}}(t')dt'\right]^2.\end{aligned} \tag{2.63}$$

From the Final Value Theorem of the Laplace Transform,

$$\begin{aligned}\lim_{t\to\infty}\langle A^2(t)\rangle &= \langle A^2(0)\rangle\left[\lim_{z\to 0}z\tilde{R}(z)\right]^2 + \\ &\quad + 2\langle A(0)\rangle\left[\lim_{z\to 0}z\tilde{R}(z)\right]\cdot\left[\lim_{z\to 0}z\mathcal{L}\left\{\int_0^t R(t-t')F_{\text{ext}}(t')dt'\right\}\right] + \\ &\quad + D_T\left\{1 - \left[\lim_{z\to 0}z\tilde{R}(z)\right]^2\right\} + \left[\lim_{z\to 0}z\mathcal{L}\left\{\int_0^t R(t-t')F_{\text{ext}}(t')dt'\right\}\right]^2\end{aligned} \tag{2.64}$$

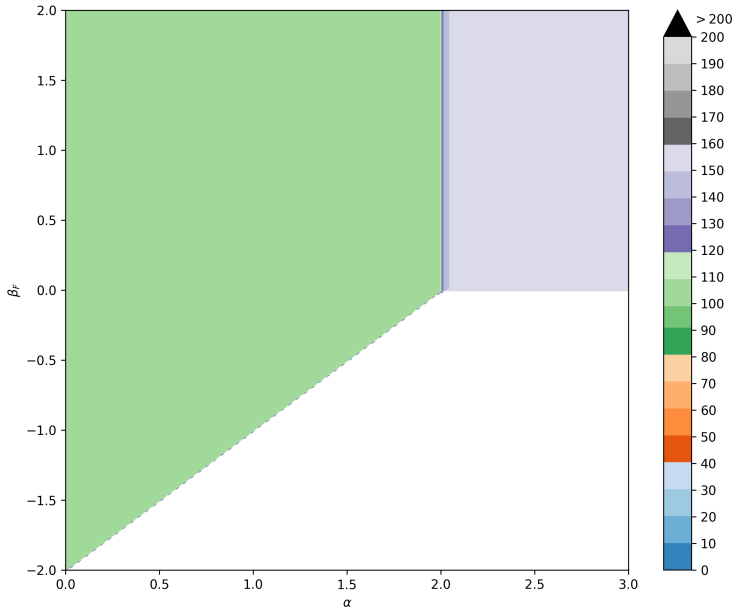

Figure 3. Stationary effective kinetic temperature $T_{\text{ef,st.}}$ as a function of the parameters α and β_F, with $z = 1.0 \times 10^{-50}$. The color scale varies from 0 to 200 arbitrary temperature units, representing the calculated values of $T_{\text{ef,st.}}$. White regions in the map indicate points where $T_{\text{ef,st.}} > 200$, signifying that the effective temperature tends to infinity under these conditions. Values used: $T_R = 100$, $T_0 = 150$, $c = 1$, $k = 1$, $mk_B = 1$, and $\langle A_0 \rangle = 0$.

or, simplifying by rearranging the terms from the convolution integrals,

$$\lim_{t\to\infty}\langle A^2(t)\rangle \;=\; D_T + \lim_{z\to 0} z^2\tilde{R}^2(z)\left[\langle A^2(0)\rangle - D_T + 2\langle A(0)\tilde{F}_{\text{ext}}(z) + \tilde{F}^2_{\text{ext}}(z)\right]. \quad (2.65)$$

By associating $\lim_{t\to\infty}\langle A^2(t)\rangle$ with the stationary effective kinetic temperature through $\lim_{t\to\infty}\langle A^2(t)\rangle = mk_BT_{\text{ef,st.}}$ and using Eqs. (2.25) and (2.49), we find

$$T_{\text{ef,st.}} \;=\; T_R + \lim_{z\to 0}\frac{1}{(1+c_Tz^{\alpha-2})^2}\left\{T_0 - T_R + \frac{1}{mk_B}\left[2\langle A(0)\rangle + kz^{\beta_F}\right]kz^{\beta_F}\right\}. \quad (2.66)$$

where we have set $D_T = mk_BT_R$, as expected in the absence of external forces and for long-time values of $R(t)$. Additionally, $T_0 = \langle A^2(0)\rangle/(mk_B)$.

Figure 3 illustrates how different combinations of α and β_F affect the thermal behavior of the system, highlighting regions of thermal stability and instability. Values used: $T_R = 100$, $T_0 = 150$, $c_T = 1$, $k = 1$, $mk_B = 1$, and $\langle A(0)\rangle = 0$. The white regions in the map indicate points where $T_{\text{ef,st.}} > 200$, signifying that the effective temperature tends to infinity under these conditions. In such cases, as previously noted, the approach based on the Generalized Langevin Equation does not apply.

2.6 Generalized Fluctuation-Dissipation Theorem

Analogously to the procedure adopted in Section 2.2, we can derive a generalization of the Fluctuation-Dissipation Theorem from the variance relation, Eq. (2.13), using Eqs. (2.40) and (2.47). Thus,

$$\begin{aligned}\sigma^2_{A^\dagger}(t) &= \left\langle A^{\dagger 2}(t)\right\rangle - \left\langle A^\dagger(t)\right\rangle^2 \\ &= \sigma^2_{A^\dagger}(0)R^2(t) + D_T\left[1 - R^2(t)\right].\end{aligned} \tag{2.67}$$

Similarly, the variance for $A^2(t)$ can be obtained. From Eqs. (2.60) and (2.62), we have

$$\sigma^2_A(t) = \sigma^2_A(0)R^2(t) + D_T\left[1 - R^2(t)\right]. \tag{2.68}$$

Since $\sigma^2_A(0) = \sigma^{\dagger 2}_A(0)$, it follows that $\sigma^2_A(t) = \sigma^{\dagger 2}_A(t)$, demonstrating that the fluctuations of $A(t)$ are independent of the presence of an external force.

Taking the limit $t \to \infty$, we obtain the value of D_T:

$$D_T = \frac{\sigma^2_{A,\text{st.}} - \sigma^2_A(0)R^2_\infty}{1 - R^2_\infty}. \tag{2.69}$$

If the system satisfies Khinchin's Theorem, then $\lim_{t\to\infty} R(t) = R_\infty = 0$ (for $0 < \alpha < 2$), restoring thermal equilibrium regardless of the initial conditions. In this case, the classical fluctuation-dissipation theorem is recovered. From relation (2.45), it follows that

$$C_\xi(t) = 2mk_BT_R\Gamma(t), \tag{2.70}$$

assuming $\sigma^2_{A,\text{st.}} = \langle A^2\rangle_{\text{st.}} = 2mk_BT_R$ and $\langle A\rangle_{\text{st.}} = 0$. This expression generalizes the result of Eq. (2.21), and by considering $\Gamma(t-t') = 2\gamma\delta(t-t')$, we recover exactly Eq. (2.21), showing the transition from the Markovian regime to its non-Markovian extension.

On the other hand, if $R(t)$ does not decay to zero at long times, i.e., $R_\infty \neq 0$, the fluctuation-dissipation relation takes on a modified form, with the term D_T, Eq. (2.69), adjusting the balance between the noise correlation $C_\xi(t-t')$ and the memory function $\Gamma(t-t')$:

$$\langle\xi(t')\xi(t'')\rangle = \frac{\sigma^2_{A,\text{st.}} - \sigma^2_A(0)R^2_\infty}{1 - R^2_\infty}\Gamma(t), \tag{2.71}$$

which extends the validity of relation (2.70) to the ballistic diffusion regime [20]. However, in the hyperballistic regime ($\lim_{t\to\infty} R(t) = 1$), it is not possible to establish a fluctuation-dissipation relation in the simple form $D_T\Gamma(t)$, as the constant D_T cannot be defined from Eq. (2.68).

To understand the role of the external force, we analyze

$$\sigma^2_{\text{st.}} = 2mk_BT_{\text{eff.}} - \left[\lim_{t\to\infty}\langle A(t)\rangle\right]^2, \tag{2.72}$$

assuming that the external force has, in Laplace space, an asymptotic behavior for $z \to 0$ of the form $\tilde{F}_{\text{ext}}(z) \sim kz^{\beta_F}$. Thus, Eq. (2.60) provides

$$\lim_{t\to\infty} \int_0^t R(t-t')F_{\text{ext}}(x,t')dt' = \lim_{z\to 0} \frac{kz^{\beta_F}}{1+cz^{\alpha-2}}, \tag{2.73}$$

where we used the Final Value Theorem and the relation $\tilde{\Gamma}(z) \sim cz^{\alpha-1}$ [76]. By analyzing the exponents, we can define conditions for the cancellation of the drift effect, depending on the values of k, β_F, and α.

If $\alpha < 2$, then $z^{\alpha-2} \to \infty$ as $z \to 0$, implying that

$$\frac{kz^{\beta_F}}{1+c_T z^{\alpha-2}} \sim \frac{k}{c_T} z^{\beta_F-\alpha+2}.$$

For the limit to be zero, $\beta_F > \alpha - 2$. In the ballistic case ($\alpha = 2$): (1) if $\langle A(0)\rangle \neq 0$, the drift effect vanishes if $k = -\langle A(0)\rangle$ for $\beta_F = 0$; (2) if $\langle A(0)\rangle = 0$, the drift $\langle A(t)\rangle$ can be canceled by choosing $\beta_F > 0$ or even in the absence of an external force. Although it is not possible to construct a fluctuation-dissipation relation for the hyperballistic regime, the disappearance of the drift can be achieved under conditions analogous to those of the ballistic case.

For values $R_\infty \neq 0$, which occurs for $\alpha \geq 2$, we have:

$$\lim_{t\to\infty} \langle A(t)\rangle = \lim_{z\to 0} \frac{\langle A(0)\rangle + kz^{\beta_F}}{1+c_T z^{\alpha-2}}. \tag{2.74}$$

In the ballistic case: 1. If $\beta_F > 0$, $\lim_{t\to\infty}\langle A(t)\rangle = \langle A(0)\rangle/(1+c_T)$; 2. If $\beta_F = 0$, $\lim_{t\to\infty}\langle A(t)\rangle = (\langle A(0)\rangle + k)/(1+c)$; and 3. If $\beta_F < 0$, $\lim_{t\to\infty}\langle A(t)\rangle = \infty$.

In the hyperballistic regime, drift effects are observed for: 1. if $\beta_F > 0$, $\lim_{t\to\infty}\langle A(t)\rangle = \langle A(0)\rangle$; 2. if $\beta_F = 0$, $\lim_{t\to\infty}\langle A(t)\rangle = \langle A(0)\rangle + k$; and 3. if $\beta_F < 0$, $\lim_{t\to\infty}\langle A(t)\rangle = \infty$.

Thus, the detailed analysis of diffusive regimes — subdiffusive, normal, superdiffusive, ballistic, and hyperballistic — and their corresponding fluctuation-dissipation relations enables a deeper understanding of the degree of generalization achieved, as well as the critical influence of the memory function, the behavior of the external force, and the decay (or lack thereof) of $R(t)$. By extending the traditional fluctuation-dissipation theorem to non-Markovian scenarios and anomalous transport regimes, we reveal the intrinsic complexity of these systems. The results presented here provide a unified conceptual framework that not only recovers well-known limits, such as classical diffusion, but also sheds light on new physical domains, where the structure of correlations, the form of the memory function, and the nature of the external force play fundamental roles in determining the stationary state of the system.

Below, we present a revised version of the text, aiming for greater fluidity, notational consistency, and clarity. Additionally, at the end, we analyze the application of the Final Value Theorem of the Laplace Transform for the evanescent force, relating it to the temporal behavior of a particle subjected to this type of field.

2.7 Force Due to Evanescent Waves

At nanoscale distances, heat transport mediated by electromagnetic fields can surpass the limit imposed by Planck's law for blackbody radiation, revealing new regimes of energy transfer [5, 87, 54]. The proximity between surfaces, typically in the near-infrared range, known as the near-field regime, allows the exploration of evanescent modes—resulting from total internal reflection or the excitation of surface polaritons—to enhance thermal conductance beyond the classical blackbody regime. These modes, confined to distances smaller than the thermal wavelength, create intense and highly inhomogeneous electric fields capable of exerting optical forces on particles or nanoparticles immersed in this environment.

Consider a planar interface located at $x = 0$ between two media: for $x < 0$, a material capable of supporting surface polariton modes; and for $x > 0$, vacuum or air. When light is incident on the medium at $x < 0$ at an angle above the critical angle for total internal reflection, the reflected wave generates an evanescent field for $x > 0$. Assuming p or s polarization and suppressing the harmonic temporal dependence $e^{-i\omega t}$, the electric component of the evanescent field can be written as

$$\mathbf{E}(x, z) = \mathbf{E}_0 e^{ik_z z} e^{-k_e x}, \tag{2.75}$$

where k_z is the wavevector parallel to the interface and $k_e = \sqrt{k_z^2 - \omega^2/c^2}$ is the imaginary component responsible for the exponential decay in the semi-space $x > 0$. This field does not propagate freely in this region but decays rapidly, generating a spatial intensity gradient near the interface. This gradient is responsible for the optical force exerted on a particle near the surface.

Now consider a nanoparticle much smaller than the wavelength of the incident light, such that the dipole approximation is valid. This particle can be characterized by an electric polarizability $\alpha(\omega)$ [35]. In response to the evanescent field, the induced electric dipole in the particle is given by $\mathbf{p} = \epsilon_0 \alpha(\omega)\mathbf{E}$. The energy stored in the dipole-field interaction and the intensity gradient of the field result in a gradient force on the particle [88]:

$$\mathbf{F} = \frac{1}{2}\mathrm{Re}\{\alpha(\omega)\}\nabla|\mathbf{E}|^2. \tag{2.76}$$

For the evanescent field given in Eq. (2.75), the field intensity is

$$|\mathbf{E}(x)|^2 = |E_0|^2 e^{-2k_e x}. \tag{2.77}$$

Consequently, the component of the force normal to the interface is

$$F_x = -\frac{1}{2}\mathrm{Re}\{\alpha(\omega)\}|E_0|^2(2k_e)e^{-2k_e x}. \tag{2.78}$$

Note that if $\mathrm{Re}\{\alpha(\omega)\} > 0$, the force is attractive towards the interface, confining the particle in an optical potential that decays exponentially with x. This optical trapping by evanescent fields is exploited in nanoscale optical manipulation experiments [89].

The force described above is essentially deterministic, assuming a well-defined field. However, when considering thermal fluctuations of the electromagnetic field—crucial in the study of heat transport near interfaces—the description becomes more complex and can be addressed using the Generalized Langevin Equation formalism, which incorporates temporal memory and stochastic forces.

By introducing fluctuations and dissipation, the effective force on the particle can be expressed in terms of temporal quantities. Suppose the external force is given by

$$F_{\mathrm{ext}}(t) = \frac{1}{2}\mathrm{Re}\{\alpha(\omega)\}\nabla|E_{\mathrm{evan}}(t)|^2, \tag{2.79}$$

where $E_{\mathrm{evan}}(t)$ can be modeled as a time-dependent function (e.g., a modulated field $\sim e^{-\kappa x}\cos(\omega t)$, with $\kappa > 0$ representing spatial decay). To analyze the long-term behavior of this force, the Laplace Transform can be employed. Let $\mathcal{L}\{F_{\mathrm{ext}}(t)\} = \tilde{F}_{\mathrm{ext}}(z)$ denote the Laplace transform of the force.

As in the preceding sections, the Final Value Theorem of the Laplace Transform allows determining the asymptotic value of the force over time, if the limit exists, from the behavior of the Laplace transform of the force as $z \to 0$.

In the case of a pure evanescent wave without additional dissipation, the force may exhibit oscillatory components (e.g., if the field has a harmonic time dependence). In this scenario, the force does not necessarily reach a constant final value, potentially failing to satisfy the conditions for direct application of the theorem. In a dissipative or memory-influenced system, as described by the Generalized Langevin Equation, the effective particle dynamics can lead to damping of oscillations and a stationary state over time, for which the theorem may be applicable. If fluctuations and coupling to the thermal bath result in a stationary equilibrium, the Final Value Theorem will indicate whether the resulting force tends to zero or a constant value as $t \to \infty$.

As an illustrative example, consider the external force exerted on a particle by an evanescent field of the form

$$F_{\mathrm{ext}}(t) = F_0 e^{-\kappa x}\cos(\omega t),$$

where $F_0 > 0$ is a constant depending on the electric field intensity and the particle's polarizability, $\kappa > 0$ characterizes the spatial decay of the evanescent field normal to the interface, and ω is the oscillation frequency of the field.

This expression describes a temporally oscillating force with spatial decay but no temporal decay. For a particle held at a fixed distance x from the interface, the force merely oscillates without reaching a constant value as $t \to \infty$. Thus, if we analyze the

Laplace Transform of this force in time,

$$\mathcal{L}\{F_{\text{ext}}(t)\} = \int_0^\infty F_0 e^{-\kappa x}\cos(\omega t)e^{-zt}\,dt,$$

we obtain

$$\tilde{F}_{\text{ext}}(z) = F_0 e^{-\kappa x}\frac{z}{z^2+\omega^2}.$$

More specifically, the Laplace Transform of $\cos(\omega t)$ is $\mathcal{L}\{\cos(\omega t)\} = \frac{z}{z^2+\omega^2}$, leading to

$$\tilde{F}_{\text{ext}}(z) = F_0 e^{-\kappa x}\frac{z}{z^2+\omega^2}.$$

Applying the Final Value Theorem gives

$$\lim_{t\to\infty} F_{\text{ext}}(t) = \lim_{z\to 0}\frac{z^2}{z^2+\omega^2} = 0.$$

Thus, $\lim_{t\to\infty} F_{\text{ext}}(t) = 0$. However, it is important to note that this result does not imply temporal stability of the force—it continues to oscillate in time and does not approach a constant value. The Final Value Theorem does not directly apply to purely oscillatory functions without damping. The above analysis simply shows that, if we attempt to use the theorem in this simple case, the indicated limit would be zero, which does not reflect a stable asymptotic state but rather the inability to extract a nonzero final value from a strictly oscillatory function.

For a nonzero final value to be obtained, damping must be introduced into the system, for instance, through a dissipative term in the field or the particle's dynamics. In this case, the external force could be modified to something like:

$$F_{\text{ext}}(t) = F_0 e^{-\kappa x}e^{-\gamma t}\cos(\omega t),$$

with $\gamma > 0$ representing a temporal decay factor. Now, applying the same procedure, the effective force will decay exponentially over time, and the Final Value Theorem can indicate the value to which $F_{\text{ext}}(t)$ tends. In this case, it will unambiguously be zero, reflecting a stationary state free from oscillations.

2.8 Temporal Behavior of the Response Function $R(t)$

We now turn our attention to the analysis of the temporal behavior of the response function $R(t)$, a key element in understanding how physical systems respond to small external perturbations. The temporal response function is an essential tool for investigating how the system evolves from a state of nonequilibrium, and it is fundamental to the formulation of various results obtained previously.

Based on the expressions describing the dynamics of temperature and the generalization of the fluctuation-dissipation theorem, we can relate the response function to other

physical quantities of the system. Thus, the expression for $R(t)$ will be used to describe the relationship between internal fluctuations and dissipation, complementing the previously developed results on stochastic dynamics.

First, we establish the relationship between the memory function and the density of states. We begin with the fluctuation-dissipation theorem in the form of relation (2.71), defined in the time domain as

$$\langle \xi(t)\xi(t')\rangle = D_T\Gamma(t-t').$$

In Fourier space, the noise correlation function is given by

$$\langle \xi(\omega)\xi(\omega')\rangle = D_T\Gamma(\omega-\omega'),$$

where $\Gamma(\omega-\omega')$ is the memory function in the frequency domain, describing frequency-dependent dissipation.

To simplify the manipulation, we introduce the variables $T = \frac{t+t'}{2}$ (mean time) and $\tau = t - t'$ (time difference). Thus,

$$t = T + \frac{\tau}{2}, \quad t' = T - \frac{\tau}{2}.$$

Substituting these variables into the Fourier correlation expression, we obtain

$$\omega t + \omega' t' = (\omega+\omega')T + \frac{\tau}{2}(\omega-\omega').$$

With this transformation, the correlation function can be rewritten as a double integral over the frequencies ω and ω':

$$\langle \xi(t)\xi(t')\rangle = \int_{-\infty}^{\infty}\frac{d\omega}{2\pi}\int_{-\infty}^{\infty}\frac{d\omega'}{2\pi}\langle \xi(\omega)\xi(\omega')\rangle e^{-i[(\omega+\omega')T+(\omega-\omega')\frac{\tau}{2}]}. \tag{2.80}$$

For a stationary ensemble, $\langle \xi_\omega \xi_{\omega'}\rangle = 0$ unless $\omega+\omega' = 0$, resulting in

$$\langle \xi_\omega \xi_{\omega'}\rangle = 2\pi S(\omega)\delta(\omega+\omega'), \tag{2.81}$$

where $S(\omega)$ is the power spectrum. Substituting this into Eq. (2.80), we obtain

$$\langle \xi(t)\xi(t')\rangle = \int_{-\infty}^{\infty}\frac{d\omega}{2\pi}S(\omega)e^{-i\omega(t-t')}. \tag{2.82}$$

Using the parity of $S(\omega)$ and Euler's relation, we arrive at the following expression:

$$\langle \xi(t)\xi(t')\rangle = \int_{0}^{\infty}\frac{d\omega}{\pi}S(\omega)\cos(\omega t). \tag{2.83}$$

We now define the density of states as

$$\rho(\omega) \equiv \frac{S(\omega)}{\pi D_T}. \tag{2.84}$$

With this, we arrive at the final expression for the memory function:

$$\Gamma(t) = \int_0^\infty d\omega \rho(\omega) \cos(\omega t). \tag{2.85}$$

In Laplace space, we have

$$\tilde{\Gamma}(z) = \int_0^\infty d\omega \frac{s\rho(\omega)}{s^2 + \omega^2}. \tag{2.86}$$

We can substitute this expression into the asymptotic behavior of Eq. (2.48):

$$\lim_{t\to\infty} R(t) = \frac{1}{1 + \int_0^\infty d\omega \frac{\rho(\omega)}{\omega^2}} = \frac{1}{1 + M_\omega}. \tag{2.87}$$

Thus, the integral M_ω is defined as

$$M_\omega = \int_0^\infty d\omega \frac{\rho(\omega)}{\omega^2}. \tag{2.88}$$

In this way, the relaxation function $R(t)$ can be determined solely from the density of states $\rho(\omega)$, which represents a crucial result of this work. The relationship between the relaxation function and the density of states allows us to directly connect the internal fluctuations of the system to dissipation, providing a solid foundation for analyzing the stochastic processes involved.

2.8.1 Temporal Behavior of the Temperature

We now proceed to analyze how the temperature evolves as a function of the relaxation function $R(t)$. From $R(t)$, we can deduce the thermal behavior of the system and relate it to the previously obtained results, deepening our understanding of thermal dynamics in the context of the Generalized Langevin Equation.

The asymptotic behavior of the effective temperature is obtained by substituting Eq. (2.87) into the temporal expression for temperature from Eq. (2.66). Considering the absence of external forces,

$$T_{\text{ef,st.}} = T_R + (T_0 - T_R) \left(\frac{1}{1 + M_\omega} \right)^2 \tag{2.89}$$

Or equivalently:

$$T_{\text{ef,st.}} = \begin{cases} T_R, & M_\omega \to \infty, \\ T_0, & M_\omega = 0, \\ T_R + (T_0 - T_R)\,(1 + c)^{-2}, & M_\omega = c. \end{cases} \tag{2.90}$$

The integral M_ω determines the system's relaxation rate and, consequently, the final state of the temperature $T_{\text{ef}}(t)$. When the integral diverges ($M_\omega \to \infty$), the memory

function does not affect the temporal evolution, resulting in complete relaxation to T_R. This indicates that the system loses influence from the initial conditions and reaches thermal equilibrium with the environment. On the other hand, when $M_\omega = 0$, the system indefinitely maintains $T(0)$, suggesting strong memory effects that prevent energy dissipation, characterizing a non-dissipative system or one without coupling to the thermal reservoir (hyperballistic case). Finally, if M_ω is a nonzero constant, the system reaches an intermediate final state, reflecting a balance between dissipation and preservation of the initial memory, resulting in a stationary local equilibrium.

2.8.2 Asymptotic Behavior of the Fluctuation-Dissipation Theorem

At this stage, we aim to infer the asymptotic behavior of the fluctuation-dissipation theorem from the relaxation function $R(t)$, considering the coupling of an external field to the system. If we can identify the behavior of D_T using Eq. (2.71), we will obtain the desired behavior for the fluctuation-dissipation theorem. By substituting Eq. (2.87) into Eq. (2.69), we have

$$D_T = \frac{\sigma^2_{A,\text{est.}} - \sigma^2_A(0)\left(\frac{1}{1+M_\omega}\right)^2}{1 - \left(\frac{1}{1+M_\omega}\right)^2} \tag{2.91}$$

such that:

$$D_T = \begin{cases} \sigma^2_{A,\text{est.}}, & M_\omega \to \infty, \\ \frac{\sigma^2_{A,\text{est.}} - \sigma^2_A(0)(1+c)^{-2}}{1-(1+c)^{-2}}, & M_\omega = c. \end{cases} \tag{2.92}$$

The analysis must be consistent with that of the temperature. When the integral ($M_\omega \to \infty$) diverges, the system is expected to lose any correlation with its initial state. Indeed, this is confirmed, as the term carrying information about the initial state vanishes under this condition. For the case of a constant and nonzero M_ω, we find intermediate values of D_T, which will be computationally discussed in subsequent sections.

Another interesting result is that, for $M_\omega \to 0$, or equivalently, $R(t \to \infty) \to 1$, it is not possible to establish a relation for D_T. Consequently, Eq. (2.71) cannot be defined. Thus, we demonstrate that, for this specific condition, the Fluctuation-Dissipation Theorem cannot be established.

3 Computational Details

In this chapter, we present the computational procedures adopted for the implementation and numerical solution of the Generalized Langevin Equation, discussed in the previous chapter. First, we address the non-dimensionalization process, aimed at reducing problem complexity and optimizing algorithm performance. Subsequently, we present the method for generating colored noise, essential for capturing the stochastic nature of Langevin dynamics and ensuring consistency with equilibrium thermodynamics. We also describe Day's method, a robust and efficient numerical technique for solving integro-differential equations, ensuring greater accuracy in simulating the complex dynamics imposed by the thermal bath.

Additionally, we analyze various physical scenarios that can be reproduced numerically, including normal diffusion, ballistic diffusion, and the influence of external potentials. The presence of an evanescent wave, particle interactions via Coulomb and elastic forces, and spatial confinement in nanoscopic environments illustrate the versatility of the proposed computational formalism.

3.1 Non-Dimensionalization

An effective way to optimize computational time is to perform the non-dimensionalization of the variables involved in the problem. This process consists of transforming the original variables into their dimensionless counterparts, eliminating the need to include physical constants in the equations during calculations. This simplification does not compromise the physical accuracy of the model, allowing the essential behavior of the system to be preserved. Once the calculations are completed, the variables can be easily reconverted to their original units, ensuring the physical interpretation of the results without loss of information.

Starting from the generalized Langevin integro-differential equation, previously described in detail in the previous chapter, we rewrite it as follows:

$$\frac{dA}{dt} = -\int dt' \, \Gamma(t - t')A(t') + \xi(t) + F_{\text{ext}}(t), \tag{3.1}$$

where $A(t) = mv(t)$ represents the canonical momentum, although it may be interpreted as any other dynamic variable in different contexts.

The memory function plays a crucial role in modeling dissipative systems. As described by Weiss [90], $\Gamma(t)$ encapsulates the interaction between the system and the

reservoir, establishing a direct connection with the spectral density of the coupling, $\rho(\omega)$:

$$\Gamma(t) = \int_0^\infty \rho(\omega)\cos(\omega t)\, d\omega,$$

as shown in Eq. (2.85). Considering a thermal bath of harmonic oscillators, the spectral density is defined as [90]:

$$\rho(\omega) = \pi \sum_a \frac{c_a^2}{2m_a\omega_a}\delta(\omega - \omega_a),$$

where c_a are the coupling coefficients and ω_a are the reservoir mode frequencies. In the continuous limit, $\rho(\omega)$ is smoothed, assuming appropriate analytical forms such as

$$\rho(\omega) = \eta\omega e^{-\omega/\omega_c},$$

where η is a dissipation coefficient and ω_c is the cutoff frequency, representing the reservoir's time scale. This relationship underpins the dissipative behavior of the system and ensures consistency with the fluctuation-dissipation theorem, as expressed in Eq. (2.70).

For the system considered above, we can introduce the stochastic force $\xi(t)$ as:

$$\xi(t) = \sqrt{\frac{2\gamma k_B T}{m}} \int d\omega \sqrt{\rho(\omega)} \cos\left[\omega t + \phi(\omega)\right], \tag{3.2}$$

where γ is the system's dissipation factor and $\phi(\omega)$ is a random function with values between 0 and 2π.

Two forms of external forces will be utilized throughout this work:

$$F_{\text{ext}}(t) = q_e E(t) + \frac{A^{(R)}}{(z_1 - z_2)^2} - B^{(A)}(z_1 - z_2), \tag{3.3}$$

where the first term refers to a usual electric force that can be adjusted to the field created by an evanescent wave [91], which plays an important role in near-field processes [32]. The second term arises from the interaction with a second particle, also immersed in the thermal bath, interacting with the first through Coulomb and elastic forces [92].

To proceed with non-dimensionalization, we start by defining a characteristic linear momentum $A_0 = mv_0$. For example, we use the molar mass of the silica molecule, SiO_2, and, based on the equipartition theorem for a free molecule in one dimension, the characteristic velocity as a function of the system's initial temperature T_0 is given by $v_0 = \sqrt{k_B T_0/m}$. The numerical values of A_0, v_0, m, and other characteristic quantities are shown in Table 2. For the characteristic time, τ, we use the inverse of the characteristic frequency ω_0, defined by the frequency of infrared radiation, which is relevant in near-field processes.

The next step is to divide both sides of Eq. (3.1) by A_0/τ. Immediately, we observe that the left-hand side becomes dimensionless:

$$\left(\frac{\tau}{A_0}\right)\frac{dA}{dt} = \frac{d\bar{A}}{d\bar{t}}; \tag{3.4}$$

Table 2. Characteristic quantities used in the model.

Quantity	**Symbol**	**Value**
Characteristic momentum	A_0	$1.44 \times 10^{-23}\,\mathrm{kg\,m\,s^{-1}}$
Mass of a SiO_2 molecule	m	9.98×10^{-26} kg
Characteristic velocity	v_0	$1.88 \times 10^{2}\,\mathrm{m\,s^{-1}}$
Characteristic force	ξ_0	$1.44 \times 10^{-11}\,\mathrm{N}$
Density of states	ρ_0	$1.00 \times 10^{12}\,\mathrm{s^{-1}}$
Dissipation factor	γ	$1.33 \times 10^{12}\,\mathrm{s^{-1}}$
Coulomb constant	$A_0^{(R)}$	$2.99 \times 10^{-31}\,\mathrm{N\ m^2}$
Elastic constant	$B_0^{(A)}$	$9.98 \times 10^{-2}\,\mathrm{N\,m^{-1}}$
External electric field	E_0^{ext}	$8.97 \times 10^{7}\,\mathrm{V\,m^{-1}}$
Characteristic length	L_0	$1.44 \times 10^{-10}\,\mathrm{m}$
Characteristic frequency	ω_0	$1.00 \times 10^{12}\,\mathrm{s^{-1}}$
Characteristic time	τ	$1.00 \times 10^{-12}\,\mathrm{s}$

we will use the symbol $\bar{X}$ over the quantity X to indicate its dimensionlessness, such as in $\bar{A}$. Now, it is necessary to ensure that the terms on the right-hand side are also independent of their dimensions. For the first term on the right-hand side, we verify that by imposing $\Gamma = 1/\tau^2\bar{\Gamma} = \Gamma_0\bar{\Gamma}$ and $\rho = \omega_0/\tau^2\bar{\rho} = \rho_0\bar{\rho}$, we ensure the non-dimensionalization of this term.

For the noise term, which has the dimension of force, we express $\xi = (A_0/\tau)\bar{\xi} = \xi_0\bar{\xi}$. Thus, it suffices to ensure that γ follows the relation:

$$\gamma = 2\left(\frac{\omega_0^2}{\xi_0^2}\right) m\rho_0 k_B T_0. \tag{3.5}$$

Finally, for the external force terms, we consider a characteristic electric field E_0^{ext}

and constants $A_0^{(R)}$ and $B_0^{(A)}$, both presented in Table 2.

The dimensionless generalized Langevin equation is:

$$\frac{d\bar{A}}{d\bar{t}} = -\int d\bar{t}'\bar{\Gamma}(\bar{t}-\bar{t}')\bar{A}(\bar{t}') + \bar{\xi}(\bar{t}) + \bar{F}_{\text{ext}}(\bar{t}). \tag{3.6}$$

3.2 Day's Method for Solving the GLE

To solve the stochastic integro-differential equation described by Eq. (3.6), we adopt the computational method proposed by James Thomas Day [93]. This method solves differential equations of the form:

$$y'(x) = f(x, y(x)) + \int_{x_0}^{x} dx' F(x', y(x')), \quad y(x_0) = y_0. \tag{3.7}$$

This equation is a particular case of the Generalized Langevin Equation, where x represents time and $y(x)$ is the generalized momentum. The generalized position can be defined as:

$$z(x) = \int_{x_0}^{x} dx' y(x'). \tag{3.8}$$

The functions involved in the process are defined as:

$$F(x', y(x')) = y(x')\Gamma(x - x'), \tag{3.9}$$

and

$$f(x, y(x)) = \xi(x) + F_{\text{ext}}(x), \tag{3.10}$$

where $\xi(x)$ represents stochastic noise and $F_{\text{ext}}(x)$ is the external force. All variables and functions in the program have been non-dimensionalized, as described in Section 3.1.

Day's method uses the trapezoidal rule for numerical integration and the approximation $y_{k+1} = y_k + h\frac{dy_k}{dx}$, assuming that time is discretized into intervals h, such that $x_{k+1} = x_k + h$. Thus, the proposed solution for $y(x)$ is given by:

$$\begin{aligned} y_{k+1} =& y_k + h\left[\frac{f(x_k, y_k) + f(x_{k+1}, y_k + hy_k)}{2}\right] \\ &+ \frac{h^2}{4}\left[F(x_k, x_0, y_0) + 2\sum_{j=1}^{k-1} F(x_k, x_j, y_j) + F(x_k, x_k, y_k)\right] \\ &+ \frac{h^2}{4}\left[F(x_{k+1}, x_0, y_0) + 2\sum_{j=1}^{k} F(x_{k+1}, x_j, y_j) + F(x_{k+1}, x_{k+1}, y_k + hy_k)\right]. \end{aligned} \tag{3.11}$$

This method also allows calculating the generalized force, derived from the linear momentum, as:

$$\begin{aligned} y'_{k+1} =& f(x_{k+1}, y_{k+1}) \\ &+ \frac{h}{2}\left[F(x_{k+1}, x_0, y_0) + 2\sum_{j=1}^{k} F(x_{k+1}, x_j, y_j) + F(x_{k+1}, x_{k+1}, y_{k+1})\right]. \end{aligned} \tag{3.12}$$

The particle's position is updated at each step by summing the average velocity in the interval, as follows:

$$z_{k+1} = z_k + h\left(y_{k+1} + y_k\right). \tag{3.13}$$

The generality of Eq. (3.7) also allows calculating the integral of Eq. (2.39), related to the response function $R(t)$:

$$\frac{dR(t)}{dt} = -\int_0^t dt' R(t')\Gamma(t' - t''), \tag{3.14}$$

where $y(x)$ becomes the response function $R(t)$, and:

$$F(x', y(x')) = R(x')\Gamma(x - x'), \tag{3.15}$$

with $f(x) = 0$.

3.3 Method for Noise Generation

Generating noise with well-defined statistical properties is a fundamental requirement in simulations of stochastic dynamics. As noted earlier, the normal Langevin equation requires delta-correlated Gaussian noise with zero mean. However, in many scenarios, a specific temporal correlation is necessary.

In the numerical scheme based on Day's method, the function $f(x, y(x))$ is decomposed into two components: a deterministic force, $F_{\text{ext}}(x)$, and a stochastic noise term, $\xi(x)$. Typically, correlated noise can be generated through the formal integration of the underlying Langevin equation. Notable examples include the Wiener process, which represents a real-valued, continuous-time stochastic process modeling Brownian motion under white noise assumptions, and the Ornstein-Uhlenbeck (OU) process, which introduces temporal correlations by applying an exponential filter to white noise. More generally, filtering a Wiener process can shape its frequency content, producing colored noise with well-defined correlation properties [67, 94].

In this work, we generate Gaussian noise with a predefined time-correlation function by implementing an algorithm originally introduced by García-Ojalvo and Sancho [95] and later adapted by Bao et al. [96]. This approach requires only the knowledge of the Fourier transform of the desired temporal correlation function. The noise is generated directly in Fourier space, rather than following a standard Wiener process. Instead, it is precomputed and incorporated as an external function in Day's method, ensuring the desired correlation properties are accurately maintained.

The starting point is to express the fluctuation-dissipation theorem in Fourier space as follows:

$$\langle \xi(\omega)\xi(\omega')\rangle = 2\pi\Gamma(\omega)\delta(\omega + \omega'), \tag{3.16}$$

where $\xi(\omega)$ and $\Gamma(\omega)$ represent the Fourier transforms of the noise and the memory function, respectively. To solve this problem numerically, we discretize the equation into N distinct time intervals, yielding the discrete relation:

$$\langle \xi(\omega_\mu)\xi(\omega_\nu)\rangle = \Gamma(\omega_\mu)N\Delta t\delta_{\mu+\nu,0}. \tag{3.17}$$

Here, Greek letters are used for indices in Fourier space, while Roman letters are used for indices in real space. To ensure this equation is satisfied, we define a set of complex numbers $\alpha_\mu = a_\mu + ib_\mu$, whose real and imaginary parts satisfy the following conditions:

$$\begin{cases} \langle a_\mu^2\rangle = \langle b_\mu^2\rangle = \frac{1}{2}, & \text{for } \mu = 1, 2, \ldots, N-1; \\ \langle a_\mu^2\rangle = 1, \quad \langle b_\mu^2\rangle = 0, & \text{for } \mu = N; \\ \langle \alpha_\mu \alpha_\nu\rangle = \delta_{\mu,-\nu}. \end{cases} \tag{3.18}$$

The variables a_μ and b_μ follow a normal distribution with zero mean. As a result, the desired noise is obtained as:

$$\xi(\omega_\mu) = \sqrt{N\Delta t\Gamma(\omega_\mu)}\alpha_\mu, \quad \mu = 1, \ldots, N-1, \tag{3.19}$$

and

$$\xi(\omega_0) = \Gamma(\omega_N). \tag{3.20}$$

Additionally, the memory function associated with the process can be calculated using the expression:

$$\Gamma(t_i) = \frac{\sum_{j=0}^{N_0}\langle \xi(t_j + i\Delta t)\xi(t_j)\rangle}{N_0 + 1}, \tag{3.21}$$

with $N_0 = \frac{N}{4}$.

3.4 Normal and Ballistic Diffusion

The next step in the implementation process is to define the memory function $\Gamma(t)$, which will be used in the Generalized Langevin Equation to describe the system's dynamics. Obtaining an accurate form for $\Gamma(t)$ is essential, as it determines the dissipation effects and temporal correlation in the system [76, 97].

In this work, we consider different forms of $\rho(\omega)$, each suitable for describing distinct diffusion behaviors. The specific choice of $\rho(\omega)$ directly influences the properties of the memory function $\Gamma(t)$ and, consequently, the system's dynamics.

The first choice describes the Normal Langevin Equation. For this, a constant density of states is used, as schematically shown in Figure 4. By substituting this function into Eq. (2.85) and ensuring that the cutoff frequency is sufficiently large, we obtain:

$$\Gamma(t) = \lim_{\omega_F \to \infty} 2\gamma \int_0^{\omega_f} d\omega \cos(\omega t) = 2\gamma\delta(t), \tag{3.22}$$

where γ is the dissipation factor. Thus, when the system exhibits this memory function, it corresponds to the Normal Langevin Equation case.

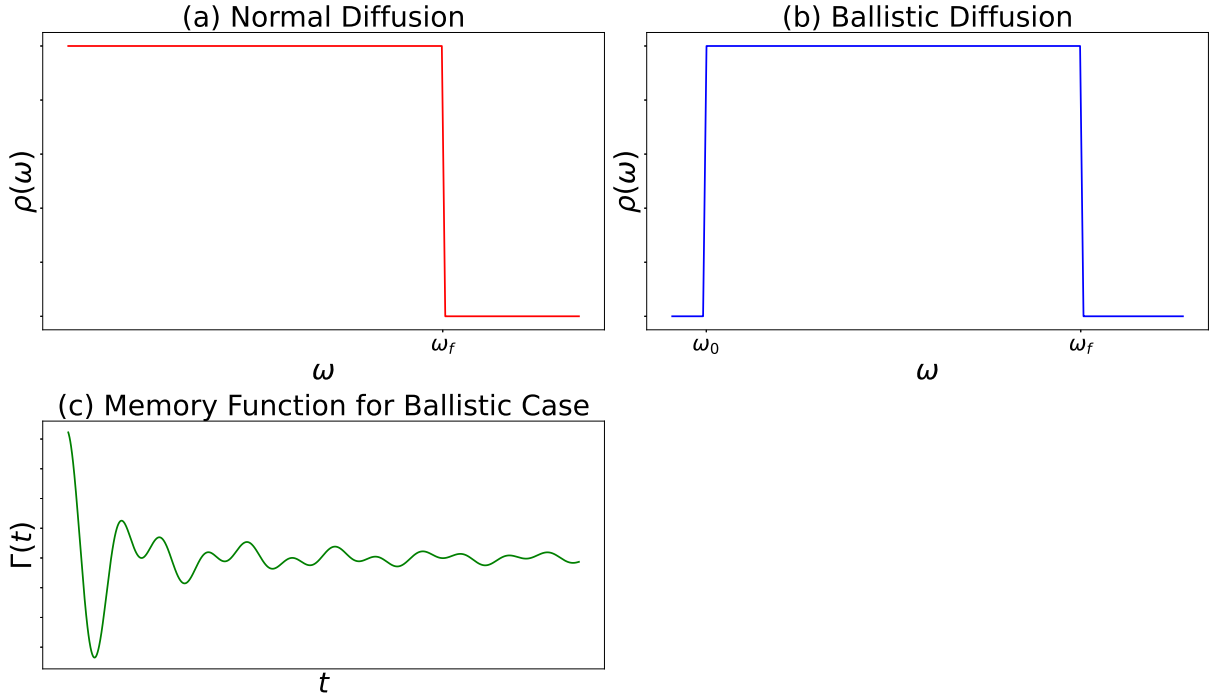

Figure 4. (a) Constant density of states function used to describe normal diffusion. (b) Constant density of states function with low-frequency modes removed, used to describe ballistic diffusion. (c) Memory function for the ballistic case.

The second choice corresponds to a case where the system has a memory function that can be calculated analytically. For this, the low-frequency modes are removed from a constant function, resulting in a step function, as shown in Figure 4. By proceeding with the integration, we have:

$$\Gamma(t) = 2\gamma \int_{\omega_0}^{\omega_f} d\omega \cos(\omega t) = 2\gamma \left[\frac{\sin(\omega_f t)}{t} - \frac{\sin(\omega_0 t)}{t} \right]. \tag{3.23}$$

This memory function is also represented in Figure 4. With this, we can describe both the Normal and Generalized Langevin Equations.

3.5 Implemented Methods

Various methods were implemented to test the Langevin equations. In addition to verification through normal and ballistic diffusion, the effects of confinement in progressively

smaller boxes, the presence of an evanescent wave, and interaction with a second particle modeled using Coulomb and elastic forces are analyzed.

3.5.1 Confinement Effect

To investigate interactions at the nanoscale, we consider a box with dimensions close to 1 nm. Based on the characteristic quantities, it was determined that 7 times the characteristic length corresponds to 1.008 nm. Therefore, the box is centered at 0, and its limit, a_{lim}, satisfies $-3.5L_0 \leq a_{\text{lim}} \leq 3.5L_0$. Our numerical method calculates the particle's position at each instant, ensuring elastic reflection at the box boundaries using the following condition:

$$\begin{cases} z = 2 \cdot a_{\text{lim}} - z, \quad v_A = -v_0, \quad \text{if } z > a_{\text{lim}}; \\ \\ z = -2 \cdot a_{\text{lim}} - z, \quad v_A = -v_0, \quad \text{if } z < -a_{\text{lim}}. \end{cases} \tag{3.24}$$

These conditions ensure that the particle reverses its direction of motion upon reaching the box's limits, keeping the system confined within the established interval. Plans include extending the method to a linear chain of particles, where the box defines the position of each particle in a coordinated manner.

3.5.2 Evanescent Wave

In a simplified manner, the first step in understanding the dynamics of an evanescent wave was to implement such a wave propagating through the box. We consider that the particle has a negative electric charge, equal in magnitude to the elementary charge. Thus, the external force can be directly obtained from the electrostatic force $F_{\text{ext}} = E_{\text{ext}}q$. The electric field used to describe the evanescent wave is given by:

$$E_{\text{ext}}(x) = e^{-\lambda\pi(a_{\text{lim}}-x)} \cos\left(kx + wt\right), \tag{3.25}$$

with:

$$k = \frac{3\pi}{a_{\text{lim}}}, \quad \text{and} \quad w = \frac{3\pi}{t_{\text{tot}}}. \tag{3.26}$$

We choose k and w so that the propagating wave makes 3 spatial oscillations and 5 temporal oscillations, where t_{tot} is the total simulation time. Additionally, $\lambda = 0.15$ is a decay factor selected to appropriately represent the problem.

3.5.3 Interaction with a Second Particle

To describe the interaction of the confined particle with a second stationary particle located at $2\,a_{\text{lim}}$, we consider that the first particle is confined in a box of size a_{lim}, as

discussed earlier. The interaction between the particles is modeled using Coulomb and elastic forces, which represents repulsive and attractive forces depending on the distance between them. The resulting interaction force is given by:

$$F_{\text{int}} = \frac{A^{(R)}}{(x_1 - x_2)^2} - B^{(A)}(x_1 - x_2), \tag{3.27}$$

where x_1 and x_2 represent the positions of the first and second particles, respectively. The first term, $\frac{A^{(R)}}{(x_1-x_2)^2}$, represents the Coulomb component of the force, dominant at short distances, while the second term, $-B^{(A)}(x_1 - x_2)$, characterizes the elastic force that intensifies at greater distances. Following non-dimensionalization, $\bar{A}^{(R)}$ and $\bar{B}^{(A)}$ are both defined in Table 2.

3.5.4 Sketch of the Simulations

Figure 5 presents a schematic representation of the implemented methods. In all simulations, the particle is constrained to one-dimensional motion. In the first configuration, the particle evolves without the influence of external forces, barriers, or additional interactions. However, two different density of states functions—normal and ballistic—are applied to compare the model with theoretical predictions.

In the three other implemented scenarios, the particle is subject to a ballistic density of states. The second scheme illustrates the effect of confinement, where a wall is positioned at coordinates $\pm a_{box}$, preventing the particle from leaving the designated region. Notably, the simulation progressively decreases the distance between the walls.

Still within the confined setup, the third simulation incorporates the interaction of the particle with an evanescent wave. It is assumed that the particle is the only charged entity within the thermal bath and, consequently, interacts with the external electric field.

Finally, in the last configuration, in addition to wall interactions, the particle interacts with a second fixed particle. This interaction occurs through Coulomb and elastic forces.

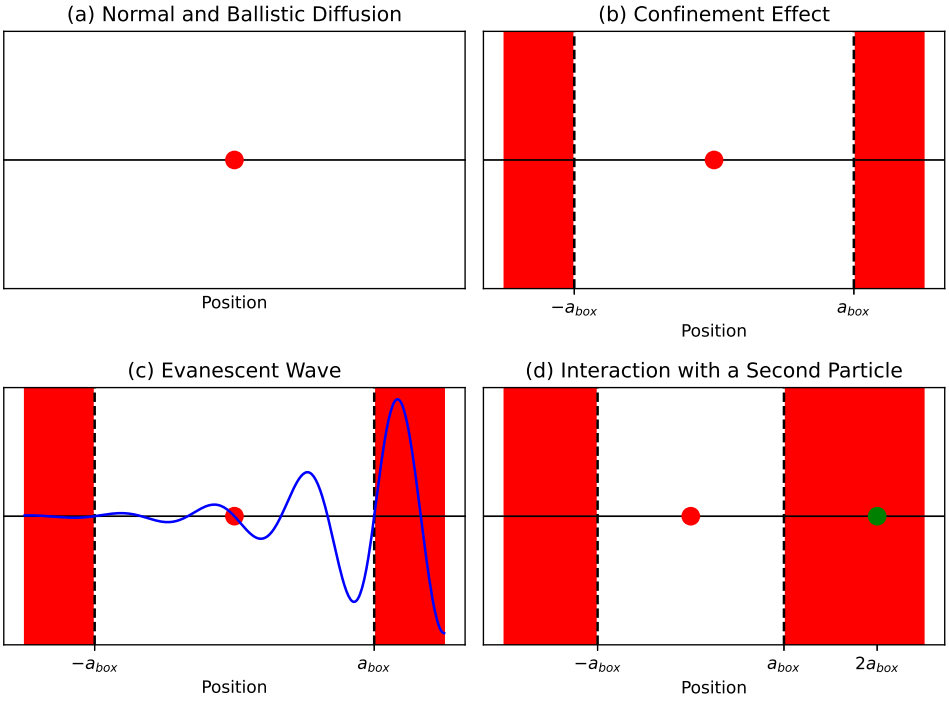

Figure 5. Sketch of the four one-dimensional simulated configurations. (a) Free motion without external forces or barriers. (b) Confinement imposed by walls at $\pm a_{box}$. (c) Interaction with an evanescent wave under confinement. (d) Interaction with a fixed second particle, in addition to the walls.

4 Computational Results

In this chapter, we present the results obtained from the computational implementations of the phenomena discussed in the previous sections. The simulations were conducted using the Python programming language, allowing for a detailed analysis of the following topics: comparison between normal diffusion and ballistic diffusion behaviors, analysis of confinement effects (box inclusion), propagation of evanescent waves, and interaction with a second particle. Each of these results will be discussed in depth, emphasizing their relevance and physical implications.

In the computational simulation, we considered a time interval from $0\,\tau$ to $15\,\tau$, corresponding to $0\,\mathrm{s}$ to $15 \times 10^{-12}\,\mathrm{s}$, subdivided into 500 identical steps. The integrations involving the angular frequency ω were performed in the range of $0\,\omega_0$ to $500\,\omega_0$, corresponding to a frequency range of $0\,\mathrm{Hz}$ to $500 \times 10^{12}\,\mathrm{Hz}$, also with 500 equal steps. To better investigate the asymptotic behavior, in some graphs, the time was extended up to $30\,\tau$, with 1000 steps, maintaining the step size consistent with the initial interval. The initial temperature was defined as $T_0 = 150\,\mathrm{K}$ and the reservoir temperature as $T_R = 100\,\mathrm{K}$.

4.1 Normal and Ballistic Diffusion

To assess the consistency of our method, we began with initial tests comparing our results with the available literature. First, we verified the correspondence of the obtained temperature with the known theoretical results. In Fig. 6, we present the temperatures for both studied cases.

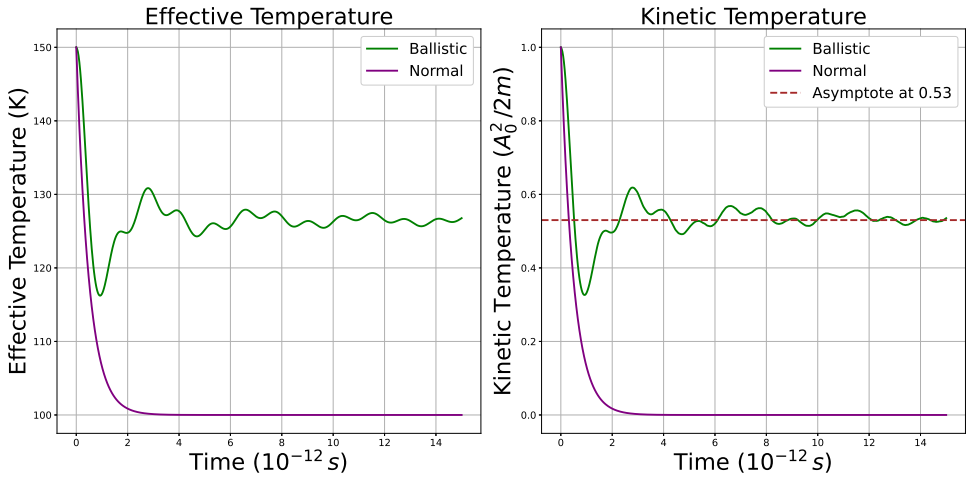

Figure 6. On the left, the effective temperature numerically calculated through Eq. (2.59). On the right, the kinetic effective temperature via simulation. **Purple line:** Normal diffusion. **Green line:** Ballistic diffusion.

On the left side of Fig. 6, the temperature is numerically calculated based on the response function, as per Eq. (2.59). In the case of normal diffusion (purple line), the temperature converges to the value of $T_R = 100\,\mathrm{K}$, indicating a dissipative domain such that the system relaxes to the reservoir temperature. This behavior is expected from Eq. (2.90), as $M_\omega \to \infty$ for the adopted $\rho(\omega)$. In the ballistic case (green line), as also predicted by Eq. (2.90), there is a tendency to stabilize at an intermediate value, which can be directly calculated using Eq. (2.89) considering the application of Eq. (2.88), with $T_{ef}(t \to \infty) = 126.5\,\mathrm{K}$.

On the right side of the figure, the comparison is made with the system's kinetic temperature through simulation. It is observed that the behavior follows the same trend presented for the effective temperature. Thus, we conclude that in both cases, the kinetic temperature adequately represents the effective temperature. Furthermore, it is possible to establish a linear scale relating both temperatures. Considering that the kinetic temperature, T_A, varies from $0\,A_0^2/2m$ to $1\,A_0^2/2m$, corresponding to an effective temperature, T_{ef}, varying from T_0 to T_R, we can express:

$$\frac{T_{ef} - T_{ef}^{(0)}}{T_{ef}^{(f)} - T_{ef}^{(0)}} = \frac{T_A - T_A^{(0)}}{T_A^{(f)} - T_A^{(0)}}.$$

Therefore,

$$T_A = \frac{T_{ef} - 100}{50}. \tag{4.1}$$

In this way, a direct method is obtained to estimate the effective temperature from the kinetic temperature. The temperature to which the ballistic case converges, on the kinetic scale, is $T_A = 0.53\,A_0^2/2m$, as presented in the respective graph.

We also analyzed the behavior of probability distributions associated with systems exhibiting anomalous diffusion, emphasizing the evolution of metrics such as skewness ($\varsigma(t)$) and kurtosis ($\eta(t)$). These indicators are crucial for characterizing the non-Gaussianity of a probability distribution and its dependence on initial conditions [21].

Skewness, measured by the obliquity $\varsigma(t)$, evaluates the degree of symmetry of the distribution and is given by:

$$\varsigma(t) \equiv \frac{\langle A^3(t)\rangle - \langle A(t)\rangle\,[3\sigma_A^2(t) + \langle A(t)\rangle^2]}{\sigma_A^3(t)}.$$

This indicator shows that if $\varsigma(0) = 0$, the initial distribution is symmetric, and this symmetry will be preserved over time, even in non-Gaussian regimes.

Kurtosis $\eta(t)$ is defined as:

$$\eta(t) \equiv \frac{\langle A^4(t)\rangle}{3\langle A^2(t)\rangle^2} - 1,$$

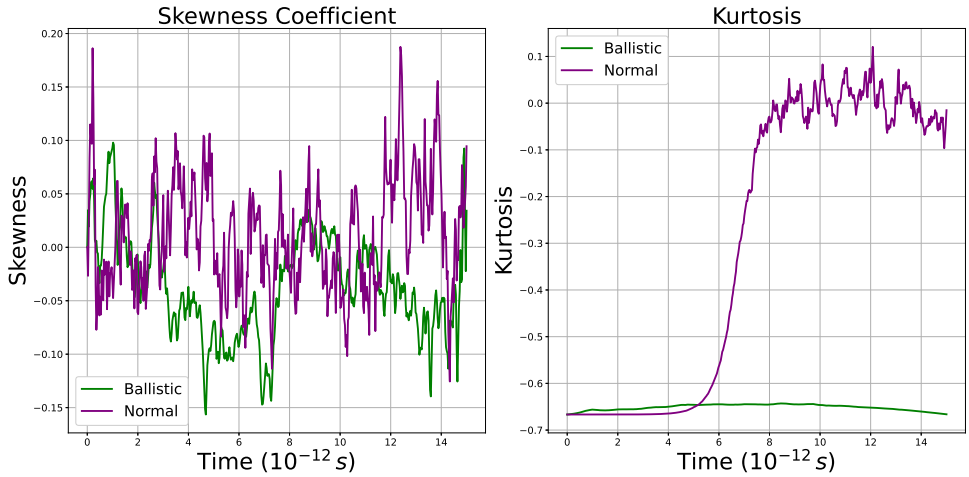

Figure 7. Temporal evolution of Skewness (left) and Kurtosis (right). **Purple line:** Normal diffusion. **Green line:** Ballistic diffusion.

and indicates deviations from Gaussianity. A distribution is considered Gaussian when $\eta(t) = 0$. For non-Gaussian distributions, $\eta(t)$ is different from zero, and its evolution directly depends on the system's memory and initial conditions.

The analyses of $\varsigma(t)$ and $\eta(t)$ were conducted based on third- and fourth-order moments, as well as variances [21]. Given that we can track the temporal evolution of positions in the presented method, we have access to the type of distribution over time. In Fig. 7, we present both coefficients for the studied cases.

For normal diffusion (purple line), a Gaussian behavior is expected, where both kurtosis and skewness tend to zero in the asymptotic regime. This behavior occurs because, in a Gaussian distribution, the tails are moderate and symmetric about the mean, reflecting the absence of temporal correlations or memory effects in the system. Indeed, as shown in Fig. 7, both coefficients approach zero over time, indicating that the distribution converges to a perfectly symmetric shape with typical tails of a Gaussian distribution, characteristic of Markovian diffusion systems.

In the ballistic case (green line), the behavior observed in the kurtosis and skewness graphs is a direct result of the influence of a long-range memory function in the diffusion system. Starting from the same condition as in normal diffusion, kurtosis in the ballistic regime begins negative, rises to a maximum, and then decreases again, suggesting that the initial memory induces flattened tails, which temporarily stabilize before diverging further from the Gaussian profile. In this case, a residual memory effect dominates the system dynamics, preventing interaction with the thermal reservoir. Skewness, on the other hand, exhibits persistent oscillations around zero, alternating between positive and negative values, revealing that the memory function also impacts the symmetry of motion, creating fluctuations that suggest a continuous directional influence periodically altering the distribution.

The results obtained show that systems with long-range memory and non-Gaussian initial conditions tend to preserve their non-Gaussianity, even in stationary states [21]. Moreover, skewness and kurtosis explicitly demonstrate the influence of initial conditions on temporal evolution, holding true for all types of diffusion regimes analyzed. These characteristics illustrate that the dynamics of systems with anomalous diffusion are profoundly influenced by correlations between stochastic variables and the system's memory.

The final verification of our method is performed through the behavior of the mean square displacement (MSD), using the Scaling Law of the MSD:

$$\langle x^2(t) \rangle \propto t^{\alpha}. \tag{4.2}$$

This relation allows us to identify the type of diffusion in the system. As previously discussed, when $\alpha = 1$, normal diffusion occurs; for $\alpha = 2$, ballistic diffusion; for $0 < \alpha < 1$, subdiffusion; and for $1 < \alpha < 2$, superdiffusion. In Fig. 8, we present the mean square displacement, along with its behavior in logarithmic scale for the last 10% of the graph, to minimize inaccuracies before stabilization.

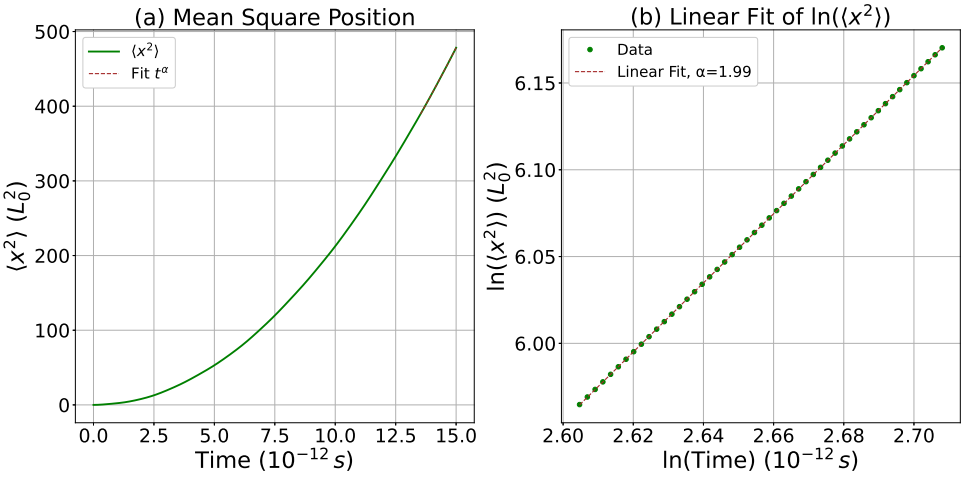

Figure 8. Mean square displacement as a function of time considering the ballistic regime. Left: linear scale. Right: logarithmic scale.

Applying the logarithm to Eq. 4.2, we obtain a linear function, whose linear regression allows the extraction of the coefficient α. For ballistic diffusion, $\alpha = 2$, consistent with the expected theoretical behavior for this type of diffusion.

4.2 Confinement Effect

Anomalous diffusion in confined systems is a widely studied phenomenon, particularly due to its implications in processes where particle motion is restricted by physical barriers or potentials. Under such conditions, the transport properties of particles can differ

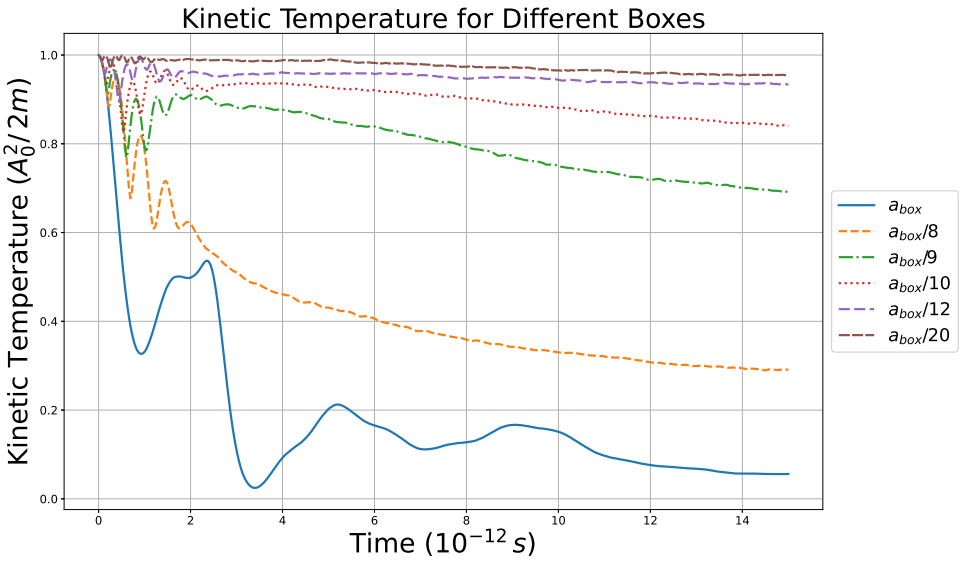

Figure 9. Temporal evolution of kinetic temperature T_A considering the confinement effect in six boxes of varying sizes. $T_A = 0$ corresponds to the thermal reservoir temperature ($T_R = 100$ K), as per Eq. (4.1).

significantly from those observed in unconfined media. The presence of solid interfaces affects the dynamics of particles near these surfaces. Using large-scale molecular dynamics simulations, Huang and Szlufarska [98] demonstrated that, near an interface, the velocity autocorrelation function of the particles—equivalent to the correlation of A—exhibits behavior significantly distinct from that of unconfined systems, significantly impacting diffusion near the interface, such that particles may experience different diffusion regimes.

To study the confinement effect, we used six boxes of varying sizes, with the reference box size defined as $a_{box} = 2\,a_{lim}$, as specified in Subsection 3.5.1. The results presented correspond to boxes with integral sizes (a_{box}) and reduced proportions, such as 1/8, 1/9, 1/10, 1/12, and 1/20 of the original size. The evolution of kinetic temperature in each configuration is shown in Fig. 9.

We observe that the kinetic temperature does not stabilize in any of the cases analyzed, which would require more computational time. However, deviations between each configuration can be identified. We also note that reducing the box size alters the behavior of this temperature: the larger the box, the closer the system approaches the reservoir temperature. It is important to emphasize that, according to the scale defined by Eq. (4.1), the zero temperature in Fig. 9 corresponds to the thermal reservoir temperature, 100 K. This suggests that larger boxes reduce interface effects, allowing for a greater proportion of interaction events between the system and the thermal reservoir. Conversely, smaller boxes hinder the system's relaxation process. As a result, the noise density of states $\rho(\omega)$ is altered such that M_ω (Eq. (2.88)) becomes even smaller, causing the relaxation function to approach 1 over long times.

4.2.1 Dissipated Power

Based on the developments presented so far, we aim to determine the dissipated power, P_{diss}, which describes how the particle exchanges energy with the thermal bath. The most direct definition for the total power is the product of the force applied on the particle, F_A, and its velocity $v(t)$, as described in Ref. [99]. In this context, we explicitly consider the canonical momentum $A(t) = mv(t)$, leading to the following expression:

$$P_{tot}(t) = F_A v(t) = \frac{1}{m}\frac{dA(t)}{dt}A(t) = \frac{1}{2m}\frac{dA^2(t)}{dt}. \tag{4.3}$$

Taking the ensemble average,

$$\langle P_{tot}(t)\rangle = \left\langle \frac{1}{m}\frac{dA(t)}{dt}A(t)\right\rangle. \tag{4.4}$$

From Eq. 2.29, we can write

$$P_{tot}(t) = \frac{1}{m}\left[-\int_0^t dt'\Gamma(t-t')A(t') + \xi(t) + F_{\text{ext}}(t)\right]A(t), \tag{4.5}$$

which, calculating the ensemble average, leads to:

$$\langle P_{tot}(t)\rangle = -\int_0^t dt'\Gamma(t-t')\langle A(t')A(t)\rangle + \langle \xi(t)A(t)\rangle + \langle F_{\text{ext}}(t)A(t)\rangle. \tag{4.6}$$

The first term on the right-hand side corresponds to the dissipated power, expressing the average energy loss from the system to the "thermal reservoir" or surrounding medium. The second term represents the fluctuating power and is related to the average contribution of noise to the work on the system variable $A(t)$. This term indicates the average energy gain or loss associated with random events, responsible for stabilizing the system in equilibrium. The third term corresponds to the external power due to the external force, whose average work per unit time is given by its correlation with the dynamic variable $A(t)$.

We are specifically interested in the dissipated power for the thermal reservoir:

$$\langle P_{diss}(t)\rangle = -\left\langle A(t)\int dt'\Gamma(t-t')A(t')\right\rangle. \tag{4.7}$$

Additionally, under the ergodic hypothesis, the time average and ensemble average can be considered equivalent, allowing greater flexibility in the analysis and interpretation of the results.

From Eq. 4.7, it is possible to estimate the dissipated power by the particles, as illustrated in Fig. 10. For the box with dimension $a_{\text{caixa}}/8$, significant fluctuations are observed at short times, suggesting the existence of a regime still underexplored, motivating future investigations and comparisons with experimental results. Overall, considering a noise density of states compatible with the ballistic regime in the unconfined case, the dissipated power oscillates around zero, highlighting the weak interaction with the thermal reservoir, as expected, even under the effect of confinement dimensions, as indicated in the temperature analysis.

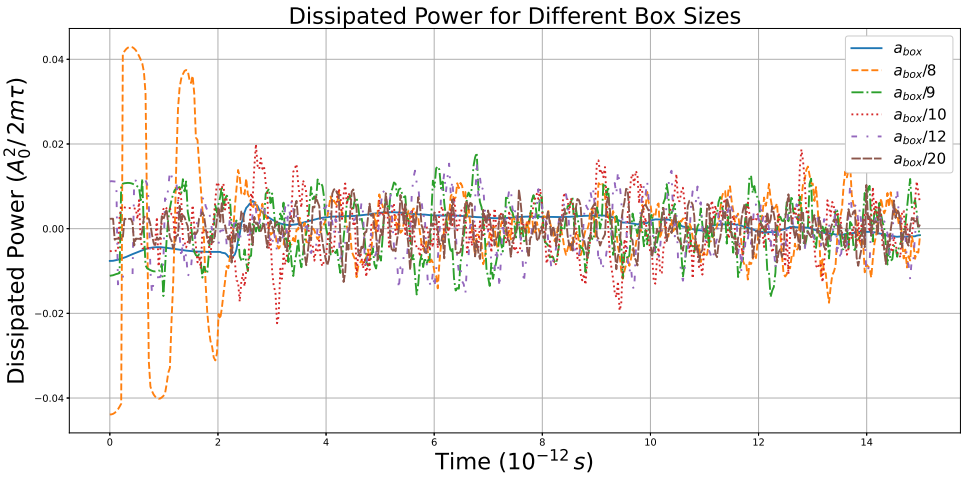

Figure 10. Dissipated power for different box sizes considering the ballistic noise density of states.

4.3 Evanescent Wave

In this section, we investigate the influence of an evanescent wave on a particle confined in a box of length a_{box}, analyzing how this external force affects the system's behavior. The starting point is the study of kinetic temperature, as illustrated in Fig. 11.

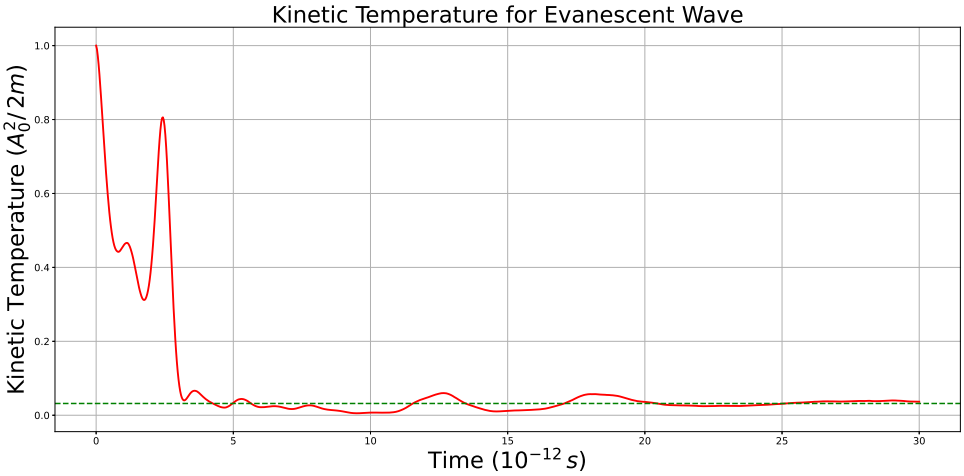

Figure 11. Kinetic temperature of a particle confined in a box subjected to an evanescent wave, considering a noise density of states consistent with the ballistic regime. The dashed green horizontal line corresponds to the kinetic temperature $T_A = 0.032\, A_0^2/(2m)$, equivalent to an effective temperature $T_{\text{ef}} = 101.6\,\text{K}$.

As in the case without an evanescent wave, the system's temperature tends toward the reservoir temperature T_R. However, in this scenario, the approach occurs more prominently and rapidly. From approximately $5 \times 10^{-12}\,\text{s}$, the temperature stabilizes, allowing the determination of a stationary kinetic temperature, $T_A = 0.032\, A_0^2/(2m)$. Using Eq. (4.1), we obtain the effective temperature $T_{\text{ef}} = 101.6\,\text{K}$, represented by the dashed green line in Fig. 11.

As previously discussed, confinement alters the stationary behavior of the relaxation function $R(t)$, resulting in a deviation of the stationary temperature compared to the case shown in Fig. 6, where $T_A = 0.53\,A_0^2/(2m)$. By using the box dimension a_{box} as a reference parameter, the system is driven to a temperature close, but not identical, to the reservoir's.

The addition of the evanescent wave exerts two main influences: 1. Reduction of the effect of the noise density of states on the stationary temperature. Although the long-range memory effect is not completely suppressed, the presence of the evanescent wave further mitigates the influence of fluctuations, enabling greater energy dissipation. 2. Acceleration of the arrival at the stationary state. Unlike the case without the evanescent wave (Fig. 6, solid blue line), where kinetic temperature stabilization is not observed within the studied time interval, the application of the evanescent wave leads the system to thermal equilibrium around 5×10^{-12} s, as shown in Fig. 11.

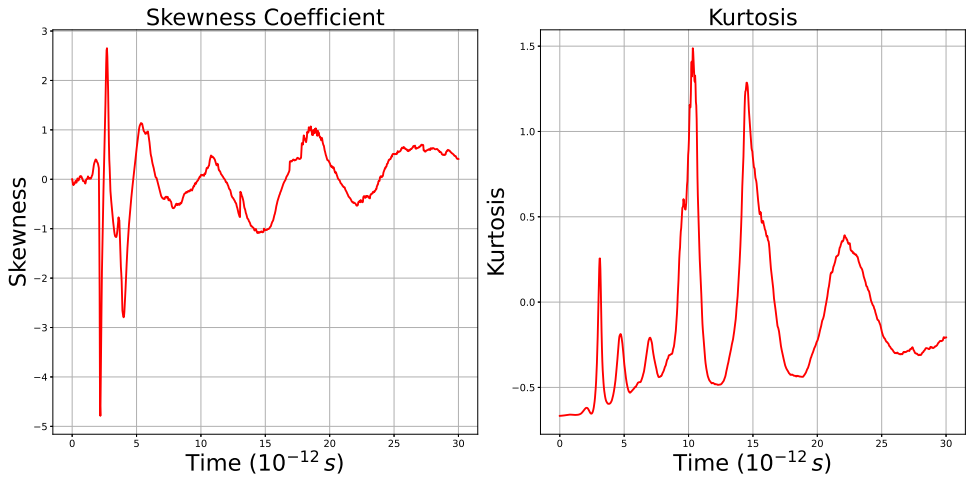

Figure 12. Skewness coefficient (left) and kurtosis (right) for the position distribution of a particle confined in a box and subjected to an evanescent wave. Stabilization of both coefficients is observed, though deviating from Gaussian behavior.

Fig. 12 shows the skewness and kurtosis coefficients. From 5×10^{-12} s onward, an apparent stabilization of the values is observed, although oscillations persist. These values can be estimated by averaging the quantities from this reference time. By doing so, we obtain a skewness coefficient of 0.095 and a kurtosis of -0.008. Thus, although the system is very close to a Gaussian distribution, residual memory effects reduce symmetry and introduce a tail to the system. It is noted that for a more detailed analysis, greater computational power would be required for simulations over a longer time scale.

Another factor corroborating the effects of the evanescent wave is the dissipated power, shown in Fig. 13. Unlike the unconfined ballistic case, where analyzed powers oscillate around zero, the power oscillations in this scenario remain above zero, highlighting the decrease in the stationary kinetic temperature at which the system stabilizes.

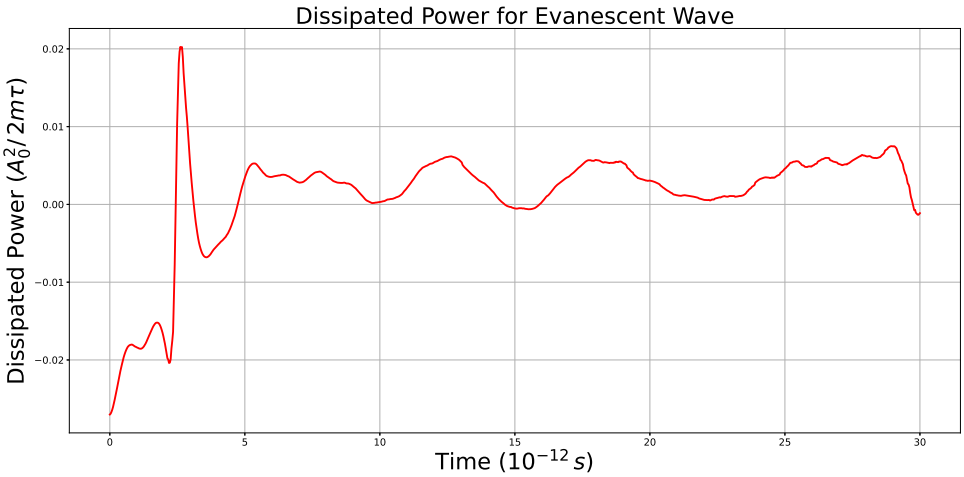

Figure 13. Dissipated power for a particle confined in a box and subjected to an evanescent wave, considering the noise density of states for the ballistic regime.

4.4 Interaction with a Second Particle

In this section, we analyze the behavior of a particle confined in a box of length a_{box}, interacting via Coulomb and elastic forces with a second particle fixed at the position $2\,a_{\text{lim}}$. The result for the confined particle's kinetic temperature is presented in Fig. 14.

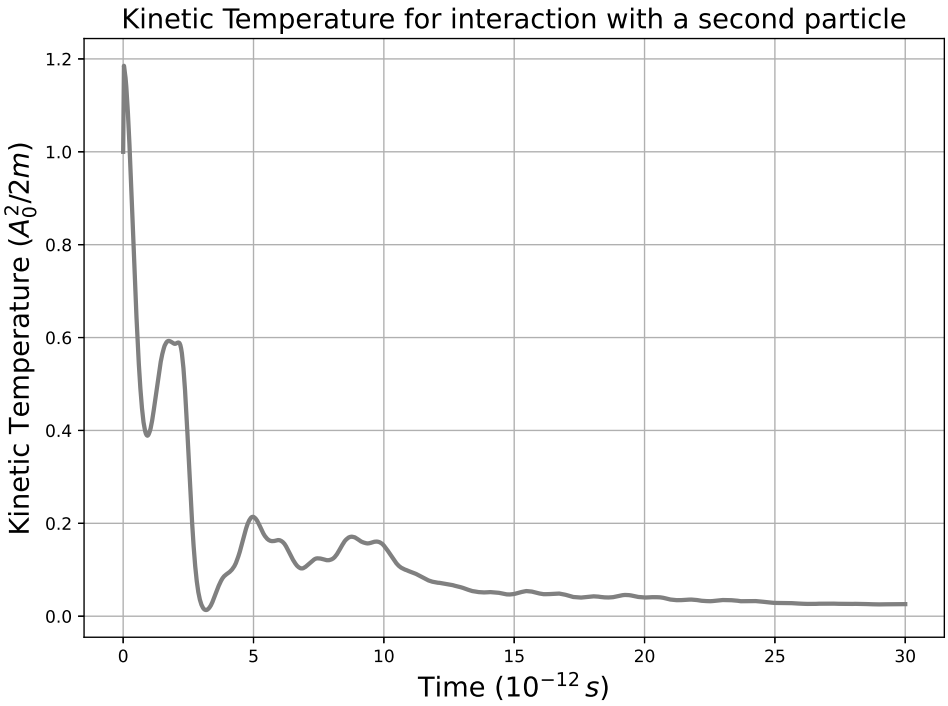

Figure 14. Kinetic temperature of a particle confined in a box interacting with a second particle via Coulomb and elastic forces, considering the same ballistic noise density of states.

As in the case without additional interaction, the kinetic temperature approaches

the thermal reservoir temperature T_R, indicating a reduction in memory effects. However, this approach is not complete: while the system progresses toward the thermal bath condition, no stationary regime is observed. Comparing this system with one without the second particle, it is evident that the external forces accelerate memory loss, resulting in a lower kinetic temperature and bringing the system closer to a quasi-thermal equilibrium regime, though not entirely.

The non-stationarity is also evident from the analysis of the system's state distribution, shown in Fig. 15. Persistent asymmetry, albeit reduced, indicates that the distribution is evolving toward a shape closer to Gaussian. The kurtosis, gradually tending to zero, reinforces this trend. Nevertheless, the distribution does not fully reach a Gaussian form within the analyzed time interval. These results suggest that while the presence of the Coulomb and elastic forces promotes memory reduction, the system does not reach a stationary state within the considered timeframe. Longer investigations, requiring greater computational resources, may be needed to confirm whether the distribution eventually stabilizes.

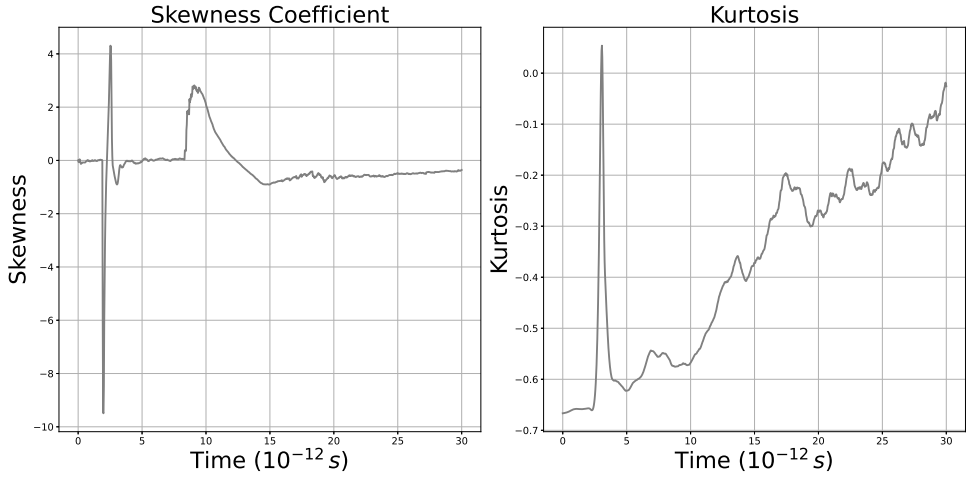

Figure 15. Skewness and kurtosis coefficients for the state distribution of a particle confined and interacting with another via Coulomb and elastic forces.

Finally, Fig. 16 shows the dissipated power in the system. We observe that the power does not stabilize over the analyzed time interval, nor does it exhibit consistent behavior indicative of convergence toward an equilibrium point. Once again, this reinforces the need for longer simulations to verify whether the system reaches a fully defined stationary regime on larger time scales.

In summary, the presence of a second particle interacting via Coulomb and elastic forces reduces memory effects and more rapidly drives the system toward the thermal bath regime, as seen in the evanescent wave case, both in terms of temperature and distribution shape. However, neither the distribution nor the dissipated power reaches a fully stationary

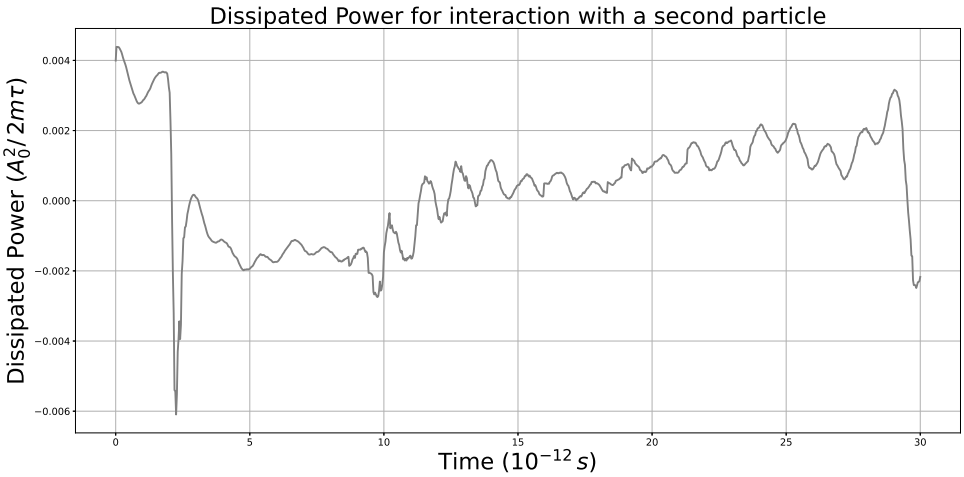

Figure 16. Dissipated power over time for the confined particle interacting via Coulomb and elastic forces. The absence of signal stabilization indicates that the stationary regime is not reached within the analyzed timeframe.

level within the considered time, suggesting that a longer-term study is necessary for definitive conclusions.

5 Conclusion

This work has yielded significant theoretical and computational results. In the initial stage of the project, we conducted an in-depth study of the fluctuation-dissipation theorem, with particular emphasis on the use of the relaxation function. This approach allowed for the identification and understanding of asymptotic behaviors related to temperature and the fluctuation-dissipation theorem itself. Subsequently, the focus shifted to the development of computational models aimed at simulating the behavior of particles in various scenarios. Several problem cases were analyzed, enabling a detailed assessment of their dynamics and implications. In this chapter, we will revisit each stage of the work, examining the objectives that motivated its development and the main results achieved.

5.1 Langevin Equation and the Fluctuation-Dissipation Theorem

The Langevin equation represented a significant milestone in understanding and advancing the theory of Brownian motion. The stochastic dynamics of systems with interactions characterized by different time scales can be robustly described by considering both emergent properties and associated memory effects. This type of description becomes even more powerful when combined with the fluctuation-dissipation theorem, which enables the determination of a system's effective temperature, even in scenarios where it never reaches thermodynamic equilibrium. This capability is particularly relevant for understanding complex systems that remain in out-of-equilibrium states, such as biological systems, disordered materials, or quantum dynamics in controlled environments. Moreover, identifying which systems exhibit such characteristics becomes crucial not only for advancing theoretical frameworks but also for practical applications, such as modeling irreversible phenomena and designing devices with tunable properties. Thus, exploring the conditions leading to these behaviors and the implications of their physical properties represents a promising path for expanding our understanding of out-of-equilibrium dynamical systems.

The first contribution of this dissertation consists of the study of memoryless systems subjected to the application of an external force. The asymptotic behavior of the Fluctuation-Dissipation Theorem in the normal diffusion regime was analyzed based on the characteristics of the Laplace transform of the external force, $F_{\text{ext}}(t)$. According to the Final Value Theorem, when $t \to \infty$, it is equivalent to considering the limit $z \to 0$ in the Laplace domain. Thus, the validity of the theorem and the introduction of correction terms, when necessary, for each type of force were presented in Section 2.2.

When $\beta_F + 1 > 0$, we have $z^{\beta_F+1} \to 0$, which satisfies the Fluctuation-Dissipation Theorem for normal diffusion. In the case where $\beta_F + 1 = 0$, the usual theorem ceases

to be applicable, making it necessary to introduce an additional correction, represented by Λ. Finally, for $\beta_F + 1 < 0$, a divergence occurs, $z^{\beta_F+1} \to \infty$, compromising both the definition of the fluctuation-dissipation relationship and the validity of the Algebraic Limit Theorem.

For the Langevin equation in the presence of a memory function, we analyzed the asymptotic behavior of the system based on the relaxation function. The analysis was also carried out in the Laplace domain, with α and β_F being the coefficients that determine the asymptotic behavior related to the type of diffusion and the external force, respectively. We demonstrated how these coefficients influence the transient and steady-state behavior of the system. Table 1 summarizes the impact of these coefficients on the steady-state behavior for different configurations.

Additionally, we determined the asymptotic effective temperature of a system from the density of states defining its memory. Based on Eq. 2.89, we demonstrated that it is possible to estimate the temperature reached by the system by evaluating the integral M_ω. For normal diffusion, the obtained result corresponds to the thermal bath temperature; for ballistic diffusion, the value lies between the system's initial temperature and the bath temperature. Notably, besides predicting this behavior, our approach allowed precise quantification of the final temperature, as validated by our computational simulations.

We also conducted an analogous analysis using the Fluctuation-Dissipation Theorem, as described in Eq. 2.91. Again, by obtaining M_ω, it was possible to determine the asymptotic behavior of the FDT, which proved consistent in both the normal and ballistic diffusion regimes. These results reinforce the robustness of our approach and its applicability in various dynamical scenarios.

5.2 Computational Simulations

The second part of the project was dedicated to simulating particles undergoing Brownian motion. To this end, we developed a method for solving the generalized Langevin equation, employing natural units after a non-dimensionalization process. The method by García and Sancho was used to generate white noise, and the integro-differential equation was solved using the trapezoidal integration method, based on Day's theory.

Initially, tests were conducted to verify the consistency of the model with existing literature and prior results. Two initial cases were analyzed: normal diffusion and ballistic diffusion. The memory for each case was generated using Eq. 2.85, with the densities represented in Figure 4. Temperature analysis showed full compatibility with Eq. 2.90. In the ballistic case, the asymptotic temperature oscillated around $126.61\,K$, indicating that the particle retains long-term memory and never equilibrates with the thermal bath. In the normal diffusion case, the particle adjusted to the bath temperature, completely

losing its initial state memory. Additionally, a linear scale relating the system's kinetic temperature to the effective temperature was established as:

$$T_A = \frac{T_{ef} - 100}{50}. \tag{5.1}$$

The next step involved confining the particle within a box, using the ballistic case's density of states. To explore nanoscale effects, the box dimension was chosen to be approximately $1\,nm$ (or $7\,L_0$ in natural units). Smaller boxes were also tested by dividing this value by 8, 9, 10, 12, and 20. It was observed that smaller boxes exhibit greater difficulty in losing initial memory. This analysis was performed based on temperature, with the $1/20\,nm$ box showing a temperature closest to the initial one, and kurtosis, which revealed a greater deviation from a Gaussian distribution.

As part of the investigation into anomalous heat transfer in near-field regimes, evanescent waves were added to the model. The ballistic density of states was maintained, and the particle was confined within a $1\,nm$ box. In this scenario, the addition of propagating evanescent waves stabilized the temperature at $101.6\,K$, slightly above the bath temperature ($T_0 = 100\,K$). This stabilization did not occur in the absence of the external electric field. Long-term memory was preserved, as indicated by the power dissipated by the system, which oscillated around a constant value greater than zero, showing that the system continuously dissipates energy into the bath.

Finally, the case connecting the model to future perspectives was explored: the interaction of the studied particle with a second one, via Coulomb and elastic forces. Once again, the particle was confined in a $1\,nm$ box, and the ballistic density of states was used. The second particle was kept stationary at $0.5\,nm$ from the boundary of the first particle's box. For the considered simulation time, stabilization of the motion was not observed. The particle's temperature tends toward the bath temperature but does not reach it, and the position distributions show a tendency toward a Gaussian shape without achieving it. Analyzing the asymptotic behavior would require greater computational power.

5.3 Future Perspectives

Future perspectives include extending the simulation time for the Coulomb and elastic interactions to understand how the particle asymptotically responds to the presence of the second particle. Additionally, we intend to allow the second particle to move freely, simulating two particles undergoing Brownian motion. This scenario will involve a high computational cost, as solving the Langevin equation for the second particle will require position-dependent interaction calculations at each time step.

Another possibility is the creation of a linear chain of particles, simulating atoms or

nanodevices. In this case, the box would represent the position of each atom or nanoparticle. The primary objective would be to investigate energy transmission along the chain, with potential extensions to energy radiation transmission processes, which are not covered in the current model.

Bibliography

[1] J. Stefan. Bulletins from the sessions of the vienna academy of sciences. *Vienna Academy of Sciences*, 79:391–428, 1879. Cited 4 times on pages 6, 7, 9, and 20.

[2] L. Boltzmann. Annalen der physik. *Annalen der Physik*, 258(6):291–294, 1884. Cited 4 times on pages 6, 7, 9, and 20.

[3] M. Planck. Ueber das gesetz der energieverteilung im normalspectrum. *Annalen der Physik*, 309(3):553–563, 1901. Cited 4 times on pages 6, 7, 9, and 20.

[4] D. Polder and M. Van Hove. Theory of radiative heat transfer between closely spaced bodies. *Physical Review B*, 4(10):3303–3314, 1971. Cited 5 times on pages 6, 7, 9, 20, and 23.

[5] A. I. Volokitin and B. N. J. Persson. Near-field radiative heat transfer and noncontact friction. *Reviews of Modern Physics*, 79(4):1291–1329, 2007. Cited 6 times on pages 6, 7, 9, 20, 24, and 48.

[6] R. Kubo, M. Yokota, and S. Nakajima. Statistical-mechanical theory of irreversible processes. ii. response to thermal disturbance. *Journal of the Physical Society of Japan*, 12:1203–1211, 1957. Cited 4 times on pages 6, 7, 9, and 20.

[7] R Kubo. The fluctuation-dissipation theorem. *Reports on Progress in Physics*, 29(1):255, jan 1966. Cited 5 times on pages 6, 7, 9, 20, and 35.

[8] H. Mori. Transport, collective motion, and brownian motion. *Progress of Theoretical Physics*, 33:423, 1965. Cited 7 times on pages 6, 7, 9, 20, 33, 34, and 35.

[9] H. Mori and H. Fujisaka. On nonlinear dynamics of fluctuations. *Progress of Theoretical Physics*, 49:764, 1973. Cited 6 times on pages 6, 7, 9, 20, 33, and 34.

[10] R. Metzler and J. Klafter. The random walk's guide to anomalous diffusion: a fractional dynamics approach. *Physics Reports*, 339(1):1–77, 2000. Cited 3 times on pages 20, 22, and 34.

[11] I. M. Sokolov. Models of anomalous diffusion in crowded environments. *Soft Matter*, 8(35):9043–9052, 2012. Cited 2 times on pages 20 and 22.

[12] R. Brown. A brief account of microscopical observations made in the months of june, july, and august, 1827, on the particles contained in the pollen of plants; and on the general existence of active molecules in organic and inorganic bodies. *Philosophical Magazine*, 4:161, 1828. Cited 2 times on pages 21 and 27.

[13] Christian Wiener. *Die Grundzüge der Weltordnung.* Book on Demand Ltd., Leipzig, 1863. Reedição de 2010. Cited on page 21.

[14] A. Einstein. Über die von der molekularkinetischen theorie der wärme geforderte bewegung von in ruhenden flüssigkeiten suspendierten teilchen. *Annalen der Physik*, 322(8):549–560, 1905. Cited on page 21.

[15] M. Smoluchowski. Zur kinetischen theorie der brownschen molekularbewegung und der suspensionen. *Annalen der Physik*, 326(14):756–780, 1906. Cited on page 21.

[16] P. Langevin. Sur la théorie du mouvement brownien. *Comptes Rendus*, 146:530–533, 1908. Cited 2 times on pages 21 and 27.

[17] N. Wiener. Differential-space. *Journal of Mathematics and Physics*, 2(1):131–174, 1923. Cited on page 22.

[18] Fernando A. Oliveira, Rogelma M. S. Ferreira, Luciano C. Lapas, and Mendeli H. Vainstein. Anomalous diffusion: A basic mechanism for the evolution of inhomogeneous systems. *Frontiers in Physics*, 7, 2019. Cited 3 times on pages 22, 40, and 42.

[19] H. B. Callen. *Thermodynamics and an Introduction to Thermostatistics*. Wiley, 2nd edition, 1985. Cited on page 22.

[20] I. V. L. Costa, R. Morgado, M. V. B. T. Lima, and F. A. Oliveira. The fluctuation-dissipation theorem fails for fast superdiffusion. *Europhysics Letters*, 63(2):173–179, 2003. Cited 4 times on pages 22, 30, 40, and 46.

[21] L. C. Lapas, I. V. L. Costa, M. H. Vainstein, and F. A. Oliveira. Entropy, non-ergodicity and non-gaussian behaviour in ballistic transport. *Europhysics Letters*, 77(3):37004, 2007. Cited 6 times on pages 22, 38, 40, 65, 66, and 67.

[22] J. Kurchan. In and out of equilibrium. *Nature*, 433(7023):222–225, 2005. Cited on page 22.

[23] S. R. de Groot and P. Mazur. *Non-Equilibrium Thermodynamics*. Dover Publications, 1984. Cited on page 22.

[24] I. Prigogine. *Introduction to Thermodynamics of Irreversible Processes*. 3rd edition, 1967. Cited on page 22.

[25] J. M. G. Vilar and J. M. Rubí. Thermodynamics "beyond" local equilibrium. *Proceedings of the National Academy of Sciences*, 98(20):11081–11084, 2001. Cited on page 23.

[26] D. Reguera, J. M. Rubí, and J. M. G. Vilar. The mesoscopic dynamics of thermodynamic systems. *The Journal of Physical Chemistry B*, 109(46):21502–21515, 2005. Cited on page 23.

[27] C. M. Hargreaves. Phys. lett. *Physics Letters A*, 30A:491, 1969. Cited on page 23.

[28] G. A. Domoto, R. F. Boehm, and C. L. Tien. Experimental investigation of radiative transfer between metallic surfaces at cryogenic temperatures. *Journal of Heat Transfer*, 92(3):412–416, 1970. Cited on page 23.

[29] R. F. Boehm and C. L. Tien. Small spacing analysis of radiative transfer between parallel metallic surfaces. *Journal of Heat Transfer*, 92(3):405–411, 1970. Cited on page 23.

[30] S. M. Rytov. *Theory of Electric Fluctuations and Thermal Radiation.* Air Force Cambridge Research Center, Bedford, MA, 1959. AFCRC-TR-59-162. Cited on page 23.

[31] S. M. Rytov, Y. A. Kravtsov, and V. I. Tatarskii. *Principles of Statistical Radiophysics 3: Elements of Random Fields.* Springer-Verlag, Berlin, Heidelberg, 1989. Cited on page 23.

[32] Jean-Pierre Mulet, Karl Joulain, Rémi Carminati, and Jean-Jacques Greffet. Enhanced radiative heat transfer at nanometric distances. *Microscale Thermophysical Engineering*, 6(3):209–222, 2002. Cited 2 times on pages 23 and 55.

[33] S.-A. Biehs. Thermal heat radiation, near-field energy density and near-field radiative heat transfer of coated materials. *The European Physical Journal B*, 58(4):423–431, 2007. Cited on page 23.

[34] Philippe Ben-Abdallah and Karl Joulain. Surface bloch waves mediated heat transfer between two nanostructured membranes. *Applied Physics Letters*, 96(14):143117, 2010. Cited on page 23.

[35] Agustín Pérez-Madrid, José M. Rubí, and Luciano C. Lapas. Heat transfer between nanoparticles: Thermal conductance for near-field interactions. *Physical Review B*, 77(15):155417, 2008. Cited 2 times on pages 23 and 48.

[36] Agustín Pérez-Madrid, Luciano Calheiros Lapas, and J. Miguel Rubí. Heat exchange between two interacting nanoparticles beyond the fluctuation-dissipation regime. *Physical Review Letters*, 103(4):048301, 2009. Cited on page 23.

[37] Ivan Latella, Svend-Age Biehs, and Philippe Ben-Abdallah. Smart thermal management with near-field thermal radiation

invited

. *Opt. Express*, 29(16):24816–24833, Aug 2021. Cited on page 23.

[38] Ivan Latella, Olivier Marconot, Julien Sylvestre, Luc G. Fréchette, and Philippe Ben-Abdallah. Dynamical response of a radiative thermal transistor based on suspended insulator-metal-transition membranes. *Phys. Rev. Appl.*, 11:024004, Feb 2019. Cited on page 23.

[39] Sheng Shen, Arvind Narayanaswamy, and Gang Chen. Surface phonon polaritons mediated energy transfer between nanoscale gaps. *Nano Letters*, 9(8):2909–2913, 2009. PMID: 19719110. Cited on page 23.

[40] Emmanuel Rousseau, Alessandro Siria, Guillaume Jourdan, Sébastien Volz, Fabio Comin, Joël Chevrier, and Jean-Jacques Greffet. Radiative heat transfer at the nanoscale. *Nature Photonics*, 3:514–517, 2009. Cited on page 23.

[41] R. S. Ottens, V. Quetschke, S. Wise, A. A. Alemi, R. Lundock, G. Mueller, D. H. Reitze, D. B. Tanner, and B. F. Whiting. Near-field radiative heat transfer between macroscopic planar surfaces. *Physical Review Letters*, 107(1):014301, 2011. Cited on page 23.

[42] Raphael St-Gelais, Biswajeet Guha, Linxiao Zhu, Shanhui Fan, and Michal Lipson. Demonstration of strong near-field radiative heat transfer between integrated nanostructures. *Nano Letters*, 14(12):6971–6975, 2014. Cited on page 23.

[43] K. Kim, B. Song, V. Fernández-Hurtado, W. Lee, W. Jeong, L. Cui, D. Thompson, J. Feist, M. T. H. Reid, F. J. García-Vidal, J. C. Cuevas, E. Meyhofer, and P. Reddy. Radiative heat transfer in the extreme near field. *Nature Nanotechnology*, 11:1–5, 2015. Cited on page 23.

[44] Jesse I. Watjen, Bo Zhao, and Zhuomin M. Zhang. Near-field radiative heat transfer between doped-si parallel plates separated by a spacing down to 200 nm. *Applied Physics Letters*, 109(20):203112, 2016. Cited on page 23.

[45] Jihong Zhang, Kezhang Shi, Lu Lu, Dudong Feng, Haotuo Liu, and Xiaohu Wu. Experiments on near-field radiative heat transfer: A review. *Clean Energy Science and Technology*, 1(1):1–35, 2023. Cited on page 23.

[46] M. Laroche, R. Carminati, and J.-J. Greffet. Near-field thermophotovoltaic energy conversion. *Journal of Applied Physics*, 100(6):063704, 09 2006. Cited on page 23.

[47] S. Basu, Z. M. Zhang, and C. J. Fu. Review of near-field thermal radiation and its application to energy conversion. *International Journal of Energy Research*, 33(13):1203–1232, 2009. Cited on page 23.

[48] Philippe Ben-Abdallah and Svend-Age Biehs. Near-field thermal transistor. *Physical Review Letters*, 112(4):044301, 2014. Cited on page 23.

[49] Ivan Latella, Svend-Age Biehs, and Philippe Ben-Abdallah. Smart thermal management with near-field thermal radiation [invited]. *OPTICS EXPRESS*, 29(16):24816–24833, AUG 2 2021. Cited on page 23.

[50] Philippe Ben-Abdallah and Svend-Age Biehs. Phase-change radiative thermal diode. *Applied Physics Letters*, 103(19):191907, 2013. Cited on page 23.

[51] Ivan Latella, Agustin Perez-Madrid, Luciano C. Lapas, and J. Miguel Rubi. Near-field thermodynamics: Useful work, efficiency, and energy harvesting. *JOURNAL OF APPLIED PHYSICS*, 115(12), MAR 28 2014. Cited on page 23.

[52] Jin Fang, Hugo Frederich, and Laurent Pilon. Harvesting nanoscale thermal radiation using pyroelectric materials. *Journal of Heat Transfer*, 132(9):092701, 2010. Cited on page 23.

[53] I. Latella and P. Ben-Abdallah. Graphene-based autonomous pyroelectric system for near-field energy conversion. *Scientific Reports*, 11:19489, 2021. Cited on page 24.

[54] Karl Joulain, Jean-Philippe Mulet, François Marquier, Rémi Carminati, and Jean-Jacques Greffet. Surface electromagnetic waves thermally excited: Radiative heat transfer, coherence properties and casimir forces revisited in the near field. *Surface Science Reports*, 57(3):59–112, 2005. Cited 2 times on pages 24 and 48.

[55] M. Terraneo, M. Peyrard, and G. Casati. Controlling the energy flow in nonlinear lattices: A model for a thermal rectifier. *Physical Review Letters*, 88(9):094302, 2002. Cited on page 24.

[56] Baowen Li, Lei Wang, and Giulio Casati. Thermal diode: Rectification of heat flux. *Physical Review Letters*, 93(18):184301, 2004. Cited on page 24.

[57] Baowen Li, Lei Wang, and Giulio Casati. Negative differential thermal resistance and thermal transistor. *Applied Physics Letters*, 88(14):143501, 2006. Cited on page 24.

[58] Luciano C. Lapas, Agustín Pérez-Madrid, and J. Miguel Rubí. Theory of casimir forces without the proximity-force approximation. *Phys. Rev. Lett.*, 116:110601, Mar 2016. Cited on page 24.

[59] Ivan Latella, Philippe Ben-Abdallah, Svend-Age Biehs, Mauro Antezza, and Riccardo Messina. Radiative heat transfer and nonequilibrium casimir-lifshitz force in many-body systems with planar geometry. *Phys. Rev. B*, 95:205404, May 2017. Cited on page 24.

[60] H. B. Chan, V. A. Aksyuk, R. N. Kleiman, D. J. Bishop, and Federico Capasso. Quantum mechanical actuation of microelectromechanical systems by the casimir force. *Science*, 291(5510):1941–1944, 2001. Cited on page 24.

[61] M. Bordag, G. L. Klimchitskaya, U. Mohideen, and V. M. Mostepanenko. *Advances in the Casimir effect*, volume 145. Oxford University Press, 2009. Cited on page 24.

[62] Biswajeet Guha, Clayton Otey, Carl B. Poitras, Shanhui Fan, and Michal Lipson. Near-field radiative cooling of nanostructures. *Nano Letters*, 12(9):4546–4550, 2012. Cited on page 24.

[63] W. A. Challener, Chubing Peng, A. V. Itagi, D. Karns, Wei Peng, Yingguo Yang, XiaoMin Yang, Xiaobin Zhu, N. J. Gokemeijer, Y.-T. Hsia, G. Ju, Robert E. Rottmayer, Michael A. Siegler, and E. C. Gage. Heat-assisted magnetic recording by a near-field transducer with efficient optical energy transfer. *Nature Photonics*, 3:220–224, 2009. Cited on page 24.

[64] Barry C. Stipe, Timothy C. Strand, Chie C. Poon, Hamid Balamane, Thomas D. Boone, Jordan A. Katine, Jui-Lung Li, Vijay Rawat, Hiroaki Nemoto, Akemi Hirotsune, Olav Hellwig, Ricardo Ruiz, Elizabeth Dobisz, Dan S. Kercher, Neil Robertson, Thomas R. Albrecht, and Bruce D. Terris. Magnetic recording at 1.5 pb m^2 using an integrated plasmonic antenna. *Nature Photonics*, 4:484–488, 2010. Cited on page 24.

[65] Robert Zwanzig. *Nonequilibrium Statistical Mechanics*. Oxford University Press, 2002. Cited 3 times on pages 25, 34, and 35.

[66] R. Kubo, M. Toda, and N. Hashitsume. *Statistical Physics II: Nonequilibrium Statistical Mechanics*, volume 31 of *Springer Series in Solid-State Sciences*. Springer-Verlag, Berlin, Heidelberg, 1985. Cited 2 times on pages 27 and 34.

[67] N. G. van Kampen. *Stochastic Processes in Physics and Chemistry*. North-Holland Personal Library. Elsevier, Amsterdam, 3rd edition, 2007. Cited 2 times on pages 27 and 58.

[68] Y. V. Prohorov and Y. A. Rozanov. *Probability Theory, Basic Concepts. Limit Theorems, Random Processes*. Springer, Berlin, 1969. Cited on page 27.

[69] Hamilton Luiz Guidorizzi. *Equações Diferenciais: Teoria e Aplicações*. LTC, 2010. Cited on page 28.

[70] E. Butkov. *Mathematical Physics*. Addison-Wesley, Massachusetts, 1968. Cited on page 28.

[71] J. L. Doob. *Stochastic Processes*. John Wiley & Sons, New York, 1990. Cited on page 30.

[72] Joel L Schiff. *The Laplace transform: Theory and applications*. Springer, New York, 1999. Cited on page 31.

[73] Emanuel Gluskin. Let us teach this generalization of the final-value theorem. *European Journal of Physics*, 24(6):591, sep 2003. Cited 2 times on pages 31 and 37.

[74] H. A. Kramers. Brownian motion in a field of force and the diffusion model of chemical reactions. *Physica*, 7:284, 1940. Cited on page 34.

[75] Peter Hänggi and Peter Jung. *Colored Noise in Dynamical Systems*, pages 239–326. John Wiley & Sons, Ltd, 1994. Cited on page 35.

[76] R. Morgado, F. A. Oliveira, G. G. Batrouni, and A. Hansen. Relation between anomalous and normal diffusion in systems with memory. *Physical Review Letters*, 89:100601, 2002. Cited 3 times on pages 37, 47, and 59.

[77] Luciano C. Lapas, Rafael Morgado, Mendeli H. Vainstein, J. Miguel Rubí, and Fernando A. Oliveira. Khinchin theorem and anomalous diffusion. *Phys. Rev. Lett.*, 101:230602, Dec 2008. Cited 3 times on pages 38, 40, and 43.

[78] Carl M. Bender and Steven A. Orszag. *Advanced Mathematical Methods for Scientists and Engineers I: Asymptotic Methods and Perturbation Theory*. Springer, New York, 1999. Cited on page 39.

[79] Rogelma M. S. Ferreira, Luciano C. Lapas, and Fernando A. Oliveira. General scaling relations in anomalous diffusion. *Acta Physica Polonica A*, 44(5):1085–1097, 2013. Cited on page 39.

[80] R. Morgado, I. V. L. Costa, and F. A. Oliveira. Normal and anomalous diffusion: ergodicity and fluctuation-dissipation theorem. *Acta Physica Polonica B*, 35:1359–1365, 2004. Cited on page 40.

[81] M. H. Vainstein, I. V. L. Costa, R. Morgado, and F. A. Oliveira. Non-exponential relaxation for anomalous diffusion. *Europhysics Letters*, 73(5):726, jan 2006. Cited on page 40.

[82] U. Agrawal, S. Gopalakrishnan, and R. Vasseur. Generalized hydrodynamics, quasiparticle diffusion, and anomalous local relaxation in random integrable spin chains. *Physical Review B*, 99(17), 2019. Cited on page 40.

[83] A. M. Jayannavar and N. Kumar. Nondiffusive quantum transport in a dynamically disordered medium. *Phys. Rev. Lett.*, 48:553–556, Feb 1982. Cited on page 40.

[84] Leonardo Golubović, Shechao Feng, and Fan-An Zeng. Classical and quantum superdiffusion in a time-dependent random potential. *Phys. Rev. Lett.*, 67:2115–2118, Oct 1991. Cited on page 40.

[85] Liad Levi, Yevgeny Krivolapov, Shmuel Fishman, and Mordechai Segev. Hyper-transport of light and stochastic acceleration by evolving disorder. *Nature Physics*, 8(12):912–917, 2012. Cited on page 40.

[86] Yoav Sagi, Miri Brook, Ido Almog, and Nir Davidson. Observation of anomalous diffusion and fractional self-similarity in one dimension. *Phys. Rev. Lett.*, 108:093002, Mar 2012. Cited on page 40.

[87] Achim Kittel, Wolfgang Müller-Hirsch, Jürgen Parisi, Svend-Age Biehs, Daniel Reddig, and Martin Holthaus. Near-field heat transfer in a scanning thermal microscope. *Phys. Rev. Lett.*, 95:224301, Nov 2005. Cited on page 48.

[88] Lukas Novotny and Bert Hecht. *Principles of Nano-Optics*. Cambridge University Press, 2 edition, 2012. Cited on page 48.

[89] Arthur Ashkin. Optical trapping and manipulation of neutral particles usinglasers. *Proceedings of the National Academy of Sciences*, 94(10):4853–4860, 1997. Cited on page 49.

[90] Ulrich Weiss. *Quantum Dissipative Systems*. WORLD SCIENTIFIC, 4th edition, 2012. Cited 2 times on pages 54 and 55.

[91] J. D. Jackson. *Classical Electrodynamics*. Wiley, 3rd edition, 1999. Cited on page 55.

[92] M. P. Allen and D. J. Tildesley. *Computer Simulation of Liquids*. Oxford University Press, 1987. Cited on page 55.

[93] James Thomas Day. Note on the numerical solution of integro-differential equations. *The Computer Journal*, 9(4):394–395, 1967. Cited on page 57.

[94] C. W. Gardiner. *Stochastic Methods: A Handbook for the Natural and Social Sciences*. Springer, Berlim, 4 edition, 2009. Cited on page 58.

[95] J. García-Ojalvo and J. M. Sancho. *Noise in Spatially Extended Systems*. Springer-Verlag, New York, 1999. Cited on page 58.

[96] Kun Lü and Jing-Dong Bao. Numerical simulation of generalized langevin equation with arbitrary correlated noise. *Physical Review E*, 72(6):067701, 2005. Cited on page 58.

[97] T. Srokowski. Stochastic processes with finite correlation time: Modeling and application to the generalized langevin equation. *Physical Review E*, 64:031102, 2001. Cited on page 59.

[98] Kai Huang and Izabela Szlufarska. Effect of interfaces on the nearby brownian motion. *Nature Communications*, 6:8558, 2015. Cited on page 68.

[99] Herbert Goldstein, Charles P. Poole, and John L. Safko. *Classical Mechanics*. Addison-Wesley, San Francisco, 3rd edition, 2002. Cited on page 69.